PERGAMON

Engineering Fracture Mechanics 68 (2001) 1923–1960

Engineering Fracture Mechanics

www.elsevier.com/locate/engfracmech

Mechanics of ice–structure interaction

Ian J. Jordaan *

Faculty of Engineering and Applied Science, Ocean Engineering Research Centre, Memorial University of Newfoundland, St. John's, Newfoundland, Canada A1B 3X5

Received 30 September 1999; received in revised form 11 September 2000; accepted 22 September 2000

Abstract

The physical processes involved in the interaction of ice masses with offshore structures are described. For design purposes, two pressure-area relationships have been deduced, which take into account the randomness of data. The first is for local pressures, using ranked data from ship rams, resulting in a power-law decrease ($\simeq -0.7$) of pressure with design area. A second (global) pressure-area relationship with random parameters has been developed, also based on data from ship rams, with a power-law decrease ($\simeq -0.4$) of average global pressure with nominal contact area. Most of the force is transmitted through small areas termed "high-pressure zones". Observations at the medium scale indicate an extremely regular cyclic load variation in a high-pressure zone over several cycles, superimposed on less regular fluctuations. The regular cyclic activity is ascribed to dynamic activity within a layer of damaged ice adjacent to the indentor or structure, and the other reductions in load to spalling activity. The main processes in the layer are recrystallization accompanied by microfracturing near the edges of the high-pressure zones (low confining pressures), and recrystallization accompanied by pressure softening at high confinements. These processes have been reproduced in triaxial tests on polycrystalline ice, and simulated in a finite element model that incorporates damage mechanics. Fractures, spalls, and splits lead to the global reductions in average pressure. Models of flexural failure are compared to data; the results confirm the trend of measurements but further full scale calibrations are needed. © 2001 Published by Elsevier Science Ltd.

1. Introduction

At low rates of loading, the deformation of ice under stress may be modelled using viscoelastic theory. The irrecoverable (flow) term is highly nonlinear yet time dependent. As the rate of loading increases, fracture and damage, the latter encompassing the effect of microstructural change on the constitutive behaviour, become important. The irrecoverable component is particularly enhanced. The focus here is the response of ice to these higher rates found in ice–structure interactions. With regard to fracture, we deal with two main situations: first, where the fractures run to the closest free surfaces, possibly within the contact area, but are not specially induced; and second, where fractures are induced, for example in the case of icebreakers or conical structures causing flexural failure of an ice sheet. In both cases, there are areas

* Tel.: +1-709-737-8941; fax: +1-709-737-4042.
E-mail address: ijordaan@engr.mun.ca (I.J. Jordaan).

0013-7944/01/$ - see front matter © 2001 Published by Elsevier Science Ltd.
PII: S0013-7944(01)00032-7

where compressive stresses are transmitted to the structure. As a guide to the indentation speeds at which brittle behaviour is observed, medium scale tests – with interaction areas of the order of a square metre – indicate ductile behaviour, nevertheless involving microstructural change, at speeds of a few millimetres per second, and brittle behaviour at higher rates.

As is the case with other materials, the strength of ice – even carefully made laboratory specimens – is several orders of magnitude less than the theoretical strength based on the separation of atoms in the crystal lattice. Ice in the field is a geophysical material, forming under natural conditions, with many pores, flaws, cracks and weaknesses. At the higher rates of interest here, these defects and flaws in the ice will intervene to cause fracture at lower stresses than ice formed in the laboratory under controlled conditions. The analysis in the present paper generally concerns ice that can represent a hazard to offshore structures, for instance multiyear ice features or icebergs; phenomena in ice sheets are also addressed. Stresses are caused by the environment, thermal as well as ocean movements such as waves. Icebergs calve, roll, and break up under gravity and buoyancy forces. At a smaller scale, the presence of vacancies, dislocations and grain boundaries in a heterogeneous grain structure cause cracks to nucleate and initiate.

The pressures within the areas where compressive forces are transmitted from the structure to the ice fluctuate considerably both in space and in time, with most of the force concentrated intensely in regions termed "high-pressure zones". An idealization of an area transmitting compressive forces is shown in Fig. 1, based on that in Jordaan et al. [1]. Within the high-pressure zones, the state of stress in the ice is triaxial, varying from low confinement near the edges to high values of contact pressure – up to 70 MPa in measurements – near the centre. There are regions of intense shear within these zones, leading to profound microstructural change in the ice. This microstructurally modified material exhibits a significantly increased compliance, compared to the "virgin" undamaged ice. At lower pressures, found near the edges of the high-pressure zones, microfracturing accompanied by recrystallization occurs, whereas the central areas of high pressure contain highly recrystallized material, the process here being aided, we believe, by pressure softening. At a certain load, the entire layer is softened and ejection of crushed ice occurs rapidly. In the earth's crust, a similar process is manifested by mylonite formation in fault zones and in areas where tectonic plates were forced together. The analogy with other geophysical materials therefore carries over to other phenomena in the earth's crust.

Ice compressive failure therefore consists of spalls, causing ice pieces of various sizes to break off, occasional splits, with the main force being transmitted through the high-pressure zones. These entities produce crushed ice consisting of quite small pieces, in prodigious quantities. Piles of crushed ice about 8 m high were observed around the Molikpaq structure during the events of March, 1986, as described by Jefferies and Wright [2]. The process is dynamic, with new spalls occurring frequently, the position and number of the high-pressure zones changing continually, leading to constant fluctuations in load and pressure. The results of medium scale experiments, [3] for example, provide important information on the nature of high-pressure zones. Full scale experiments, such as ship rams, provide invaluable data on forces and pressures. Some aspects are essentially deterministic, and others probabilistic in character (see also Jordaan and Xiao [4]). High-pressure zones will tend to locate in the most confined regions, away from the free surfaces. At the same time, they move about, responding to the occurrence of fractures, sometimes moving away from the "most likely" locations. Fractures will tend to occur where there are flaws in the ice, coupled with the location of the stress concentrations associated with the high-pressure zones themselves. Fracture and high-pressure zone formation are coupled yet distinct processes. Measurements of loads, both local and global, in the full scale, show great randomness. In using the term "random", we mean that there is uncertainty associated with the process or value under consideration. This does not mean that there are not deterministic aspects or correlations. Theories of chaotic behaviour do not relieve the designer of the necessity to deal with this uncertainty.

The factors just noted contribute to make the process of failure rather complex. If one considers the situation facing the designers of the Hibernia platform more than a decade ago, full scale observations of

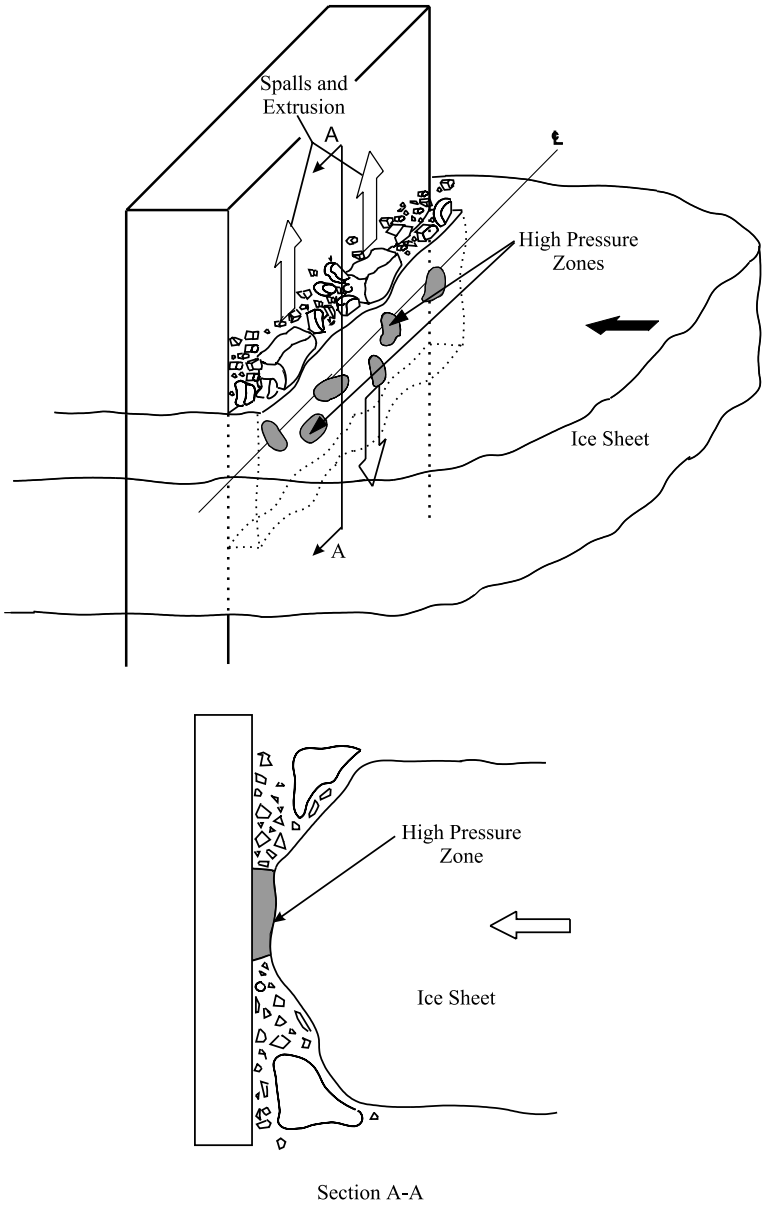

Fig. 1. Schematic illustration of the main processes of spalling, extrusion and high-pressure zone formation.

ice forces were rather limited – they still are – with no detailed observations at all of interactions of large icebergs with a structural form. Such an event has occurred, for example in the case of the Titanic, but one can only surmise the nature of the events in this incident (probably small global forces and very high local pressures causing rupture of the riveted plates). Probabilistic simulations were carried out in the case of the Hibernia design taking into account uncertainty in iceberg size, velocity and shape, but the global iceberg strength was considered to be a constant pressure of 6 MPa (design ice stresses higher than 6 MPa were

once considered necessary for design of structures in the Beaufort Sea). The resulting design force (at the 10^{-4} annual probability of exceedance) was of the order of 1700 MN. Later probabilistic simulations [5,6] have shown that, if randomness in the ice response, based on measurement, is taken into account, values as low as 400–500 MN result. In ship design, it has also been possible to reduce considerably the global load requirements [7]. In brief, it was shown that the exponent b in the expression for maximum bow force $a\Delta^b$, where Δ is displacement, could be reduced from 0.9 to 0.7. This resulted in significant reduction in bow force for larger vessels. The result was obtained by an extensive probabilistic analysis of full scale data.

Local pressures are a very important aspect of design. The specifications for the Hibernia platform included a high pressure (11 MPa) for areas of $1m^2$, diminishing to the value of 6 MPa at large areas. A detailed analysis, with the values from ship ramming as a basis, indicates that a high value is needed for small areas, but that the pressures can be reduced from the values just quoted, especially for larger areas [5,6]. The structural response is also an important consideration. For example, in steel structures where lateral support is given to a plate, membrane action can develop, providing considerable additional strength. This might involve local damage of the structure without failure, and serviceability considerations might drive the design.

The discussion just given indicates a considerable amount of uncertainty in the load estimates. In the next section, first a brief review of probabilistic modelling will be given, with emphasis on those points of importance to an understanding of the requirements in ice force modelling for design. The remainder of the paper includes a review, from the same standpoint of determination of design loads and pressures, of the physics and mechanics of the process, and to future directions.

1.1. Comments on notation

Some difficulties have been generated by the use of inconsistent notation and definitions in recent publications. In order to assist in mutual understanding, the following definitions are used in the present publication. Some might seem obvious, but it is considered important to distinguish, for example, between the usual crack initiation and a pulverization front.

- *Cleavage crack:* planar crack in ice sheet parallel to surfaces.
- *Crack initiation:* creation of new surfaces by local tensile stresses at flaws in the material. Contrast with pulverization front, defined below.
- *Damage:* softening of the material by fractures, microfractures or other microstructural changes such as recrystallization and pressure softening.
- *Extrusion:* ejection of pulverized material from edges of high-pressure zone, observed as powdered ice particles. On load upswings, the damaged layer is quite soft compared to the virgin ice, but granular particle sliding (see below) is not generally observed in a high-pressures zone until after a pulverization event (see below).
- *Granular particle sliding:* movement of particles over each other with no bonding between particles. Theories of the Mohr–Coulomb variety more appropriate than those based on viscosity.
- *High-pressure zone:* entity formed within the compressive failure region, where high concentrated pressures through highly confined ice are transmitted.
- *Pulverization:* process of disintegration following profound microstructural change in layer within high-pressure zone; ejection of ice accompanies the development of a pulverization front (see next item).
- *Pulverization front:* distinct boundary between largely undamaged ice and recrystallized, damaged, fine-grained material in high-pressure zone; essentially a slip plane developing as a result of a large mismatch of stiffness between the two material states (damaged and undamaged); crack like in appearance, and occasionally appears to follow macrocracks in the ice.
- *Spalls:* localized fractures from crack initiation occurring near high-pressure zones.

2. Probabilistic analysis

From the point of view of the designer of an offshore rig or vessel capable of resisting ice forces with adequate reliability, it is necessary to determine the ice forces, both global and local, using probabilistic methods. For example, the Canadian Standards Association (CSA) Standard S471 [8] specifies exceedance probabilities for the annual maximum load. This is illustrated in Fig. 2 for both rare and frequent loading. In the figure, the "parent" probability distribution would be that obtained, for example, by repeated rams of a vessel, yielding a statistical distribution. This could then be used to determine design loadings. This ideal situation of a set of measurements rarely exists, and generally it is necessary to massage the available data, and if necessary carry out simulations in the absence of measurements, taking into account the attendant uncertainties.

A wide range of return periods of significant events is found [6]. For the fixed structures on the Grand Banks, a large iceberg might impact the structure once every ten years. A floating system, for which measures are taken to avoid icebergs, might have a significant interaction every hundred years. These would constitute "rare" events. Calculations include consideration of the areal density of icebergs, together with detection and avoidance as a function of sea state. Some uncertainties remain with regard to the data base, but it is considered that these estimates are realistic. The piers on the Confederation Bridge might receive thousands of interactions with pressure ridges per year. These events would be considered to be "frequent". For arctic class vessels, the exposure depends on the class of the vessel, since this controls access to various ice conditions. The highest Canadian class (CAC1) is designed to deal with several thousands of rams per year, with the lowest class (CAC4) based on a smaller number, of the order of 10–20.

Given the state of knowledge as summarized in the Section 1, the most convincing approach to a design load determination is the use of full scale data, aided by an understanding of the physical processes involved. In our research programme, both local and global forces have been investigated. For illustrative purposes, the following discussion will concentrate for the most part on global forces. The measurements collected on board ships are most important. The data sets include experiments on the CCGS *Louis S. St. Laurent*, the *Canmar Kigoriak*, the *MV Arctic*, the USCGC *Polar Sea*, the SS *Manhattan*, and the *Oden*.

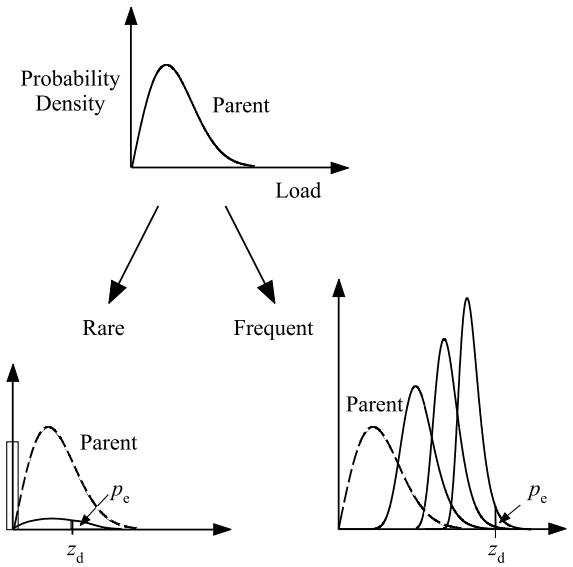

Fig. 2. Extremal analysis of random load; z_d indicates design value at probability of exceedance p_e.

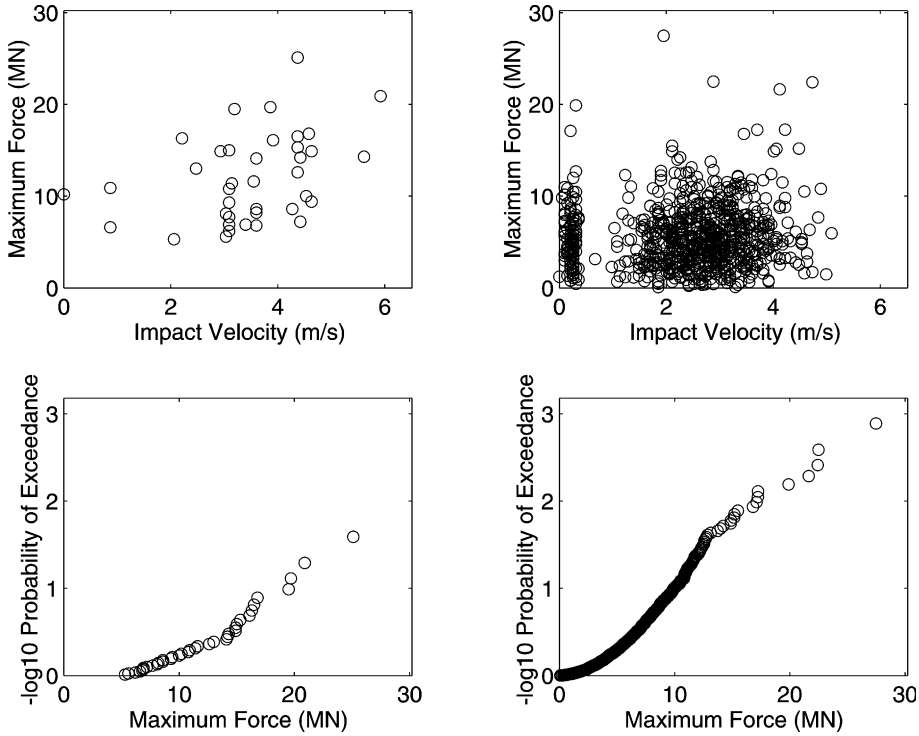

Fig. 3. (upper) Forces obtained in ramming trials (left) Polar Sea (right) Oden; (lower) data ranked and plotted to obtain probabilities of exceedance (top and bottom correspond). Similar results are found for local pressures.

Data from trials on all of these vessels have been subjected to probabilistic analysis [7,9]. Fig. 3 shows some results for two of the vessels. The first plot is from rams by the Polar Sea [10], in which flexural failures were not in evidence, while the second shows results for the Oden [11], in which they were. A feature of the results is the randomness of the data points, even under seemingly identical conditions. The randomness shown in Fig. 3 is found in very similar form, for local pressures as well.

An important point to note is the absence of any dependence on velocity, for rams above about 1–2 $m\,s^{-1}$ (data from the MV Arctic shows some velocity dependence in this range). While time-dependent effects are evident in ice indentation and fracture, the material can be rather forgiving with regard to velocity of interaction. Masterson et al. [12] found a velocity dependence of pressure in the medium scale in the range of indentor speeds from 0.1 to 100 $mm\,s^{-1}$, with the highest pressure at 3.2 $mm\,s^{-1}$. These are very low speeds for the interaction scenarios of importance in the present work. We have analysed the difference in tensile stresses adjacent to a high-pressure zone for two different rates of loading [13], in the speed range just noted, taking into account the damage process. It was concluded that the high rate of loading causes a much higher stress concentration near the high-pressure zone, thus increasing the likelihood of a spall, in agreement with observations from medium scale tests. This logic will carry through for even higher loading rates. The average local pressures on areas of the size of a square metre or more will not be sensitive to the fact that high-pressure zones are concentrated in areas of, say, 0.1 m^2, or somewhat larger or smaller areas, provided the force transmitted is the same.

It should also be noted that slow loading, of the order of a few millimetres per second, can result in very large time-dependent spalls [3,12]. This tends to mitigate the higher local pressures found under these circumstances, and also the global forces. On a statistical basis, the extreme loading at the slower rate

would, as a result, tend to reduce. Experience from the Molikpaq does not suggest that the higher loads and pressures occur at lower rates. It is considered that, for practical design, velocity effects can generally be included in the statistical analysis, except for very slow creep-type events.

How do we deal with the array of points in the upper graphs of Fig. 3? Techniques used include the bounding of the cloud of points, but then the question arises that more tests would undoubtedly raise the bound (or fewer lower it). A rational probability-based analysis is needed. The lower graphs of Fig. 3 shows the same sets of points ranked and plotted in a form of an exceedance distribution. This suggests that a distribution be fitted to these curves (this could be done for central part but for extremes we are more interested in the tail). Let the resulting cumulative distribution function be $F_X(x)$ where X is the force or pressure under consideration. As an example of application, we can often assume a Poisson arrival process of loading events [14], not necessarily with a constant arrival rate. This results in the following expression for the distribution of extreme load Z, which can be derived by writing the expression for zero arrivals in the process, with rate $v[1-F_X(z)]$, where $Z=$ extreme value, and $v=$ number of arrivals in a year, taking this period as the interval of interest.

$$F_Z(z) = \exp\{-v[1 - F_X(z)]\}. \tag{1}$$

The choice of period of time could be a year, as this facilitates comparison with other risk indices, or the lifetime of the structure, or any other time period that is useful for the question being studied.

Often distributions such as those in the lower part of Fig. 3 have exponential tails of the form

$$p_e = \exp[-(x - x_0)/\alpha], \tag{2}$$

where $p_e=$ probability of exceedance $=1-F_X(x)$, and x_0 and α are constants. Then Eq. (1) takes the form of the double exponential or Gumbel distribution:

$$F_Z(z) = \exp\{-\exp[-(z - x_0 - x_1)/\alpha]\}, \tag{3}$$

where $x_1 = \ln v$.

This strategy worked quite well for local pressures [15,16]. By considering the duration of each ram, one could postulate that the "exposure" to pressure was proportional to this time. Other effects, such as the size of the vessel, were included in this exposure term. When considering global loads, the peak force is strongly dependent on the vessel size; for iceberg impact with offshore structures, the mass and velocity of the iceberg is very important (limiting kinetic energy) [5]. In these cases, resort was had to Monte Carlo simulations, which formed the basis for the determination of $F_X(x)$.

But how can one reflect the considerable randomness shown in the upper part of Fig. 3? It is known that the average global pressure decreases with nominal contact area [17]. Following this work, the global average pressure P, as a function of nominal contact area a was modelled by the power-law relationship

$$P = Ca^{-D}, \tag{4}$$

where C and D are coefficients. A typical specific relationship is that due to Sanderson [17], in which the exponent D was taken as 1/2; this was consistent with a Weibull distribution of material containing random flaws. In order to deal with the randomness noted, Sanderson modelled the coefficient C as random in a design application. In our analysis of the ramming trials on vessels we took both C and D as random, so as to be able to fit all of the ship ramming data available, and extend the range of realistic physical situations. The quantities C and D were modelled using lognormal and normal distributions respectively, and consequently P is also lognormally distributed. More work remains to be done in this area, to determine the most appropriate form of distributions.

Several fits to the data were attempted; the best was found when $\mu_C = 3$ MPa, $\mu_D = -0.4$, $\sigma_C = 1.5$ MPa, $\sigma_D = 0.2$, where $\mu=$ mean, $\sigma=$ standard deviation [7,18]. The results show a general agreement with Sanderson's pressure–area relationship [17]. Fig. 4 shows a typical match between these results and

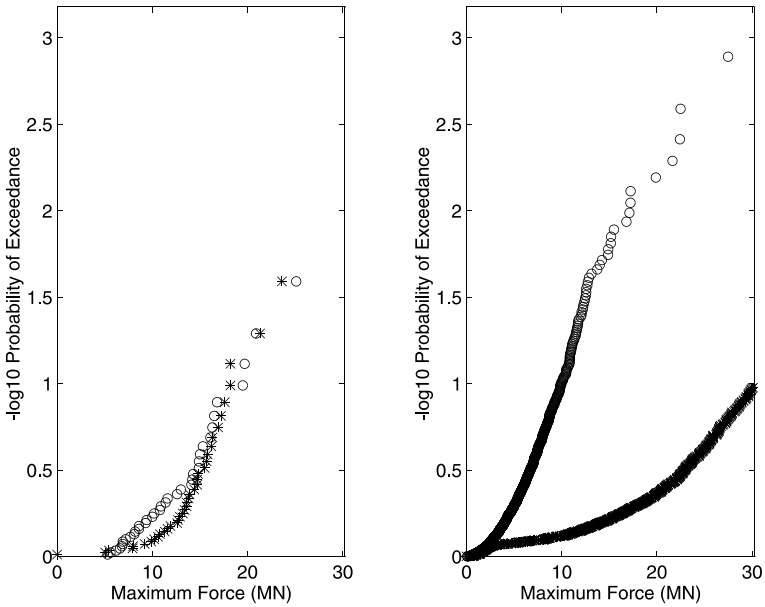

Fig. 4. Comparison of ranked data with simulation based on random C, D. Circles are the measured data, and crosses, the simulation. The agreement was generally good, as in the figure on the left (Polar Sea). The exception was the Oden (right) which regularly encountered flexural failures. See also Fig. 29.

measurement. All vessels showed good agreement except the Oden. In this case, flexural failure had to be taken into account; see Section 5.

It is important to note that the decrease of average pressure with contact area constitutes a *scale effect.* In the "classical" analysis of indentation using rigid indentors against elastic or plastic materials, the failure pressure will not depend on area. For example, the von Mises plane strain solution for the applied pressure p at failure is

$$\frac{p}{\sigma_y} = 2.97, \tag{5}$$

where σ_y is the yield stress. There is no dependence of p on area.

The design load or pressure should reflect the exposure, i.e. number of interactions per unit of time [7,19,20]. The greater the number of interactions per unit of time, the further one has to go into the tail of the parent distribution. Design naturally concentrates on extremes. Taking into account the randomness just discussed, the results will reflect the fact that in some extreme cases there would be a minimal reduction in the actual contact area with nominal contact area, if fractures do not occur, for example in a large ice feature with fewer than average flaws, and possibly free surfaces that are distant and inaccessible.

In formulating the design values [6,21], it is useful to distinguish those factors that contribute to the number of interactions as against those that affect the failure load itself. The former appear as, for example, $x_1 = \ln v$ in Eq. (3) above (where $v =$ number of arrivals in a year). The logarithmic term results in these values having a lesser significance than other parameters. Such aspects assist in finding the most important factors affecting the design load. The design load is, as noted, in the tail of the extremal (and parent) distribution. These critical cases will often correspond to those situations where spalling is minimal. This needs fracture mechanics to determine, but provides a different focus from the cases where there are many large spalls.

3. Compressive failure: nonsimultaneous aspects

As mentioned in the Introduction, there is a considerable variation in pressure across the compressive interface in ice–structure interaction. This was first recognized by Kry [22]. Further insights were provided by Ashby et al. [23], and recently by Blanchet and DeFranco [24]. Fig. 5, based on the paper by Ashby et al., illustrates the essential point rather well. It is based on the failure of a brittle wax sheet driven against a cylindrical indentor. The load at various points in time is transmitted through several distinct points; fractures and spalls result in the contact points continually changing in position. This situation calls for a probabilistic analysis; approaches to this problem have indeed been made by the authors quoted.

As noted, observations of the nonsimultaneous failure of ice were first made by Kry; further evidence is provided in the observations onboard the CCGS *Louis S. St. Laurent* by Glen and Blount [25]. Our idealization of the situation is shown in Fig. 6 for various geometries. An analysis of data from pressure measurements during ship rams has led to the conclusion that there are approximately one per m^2, on average. The average force is about 1 MN, giving an average pressure of 1 MPa. It must be emphasized strongly that these are statistical averages; the key design situations may occur when there is a strong departure from these values.

The fractures causing spalls tend to propagate to the free edges; Croasdale [26] and Croasdale et al. [27] developed first this line of thinking. As a result, there is a tendency for there to be fewer high-pressure zones near the edge of the ice feature. This is particularly evident in the case of sheets, in which the high-pressure zones are found more often near the centre of the ice sheet. This concept was introduced as a "line load" by Riska et al. [28]. Idealizations of the kind shown in Fig. 6 were presented in Jordaan et al. [1] and Jordaan and Xiao [4].

In the case of a massive ice feature, for instance a thick multiyear floe, the spalls near the edge of a high-pressure zone can propagate to points within the interaction surface (Fig. 7), resulting in a spall within the interaction area (internal spall). This kind of spall was observed in the medium scale indentation tests (see Fig. 16 and also below). The evidence suggests that the high-pressure zones do not in this case form in lines as they do in thinner ice sheets. Fig. 7 also emphasizes the importance of internal flaws in this highly random process.

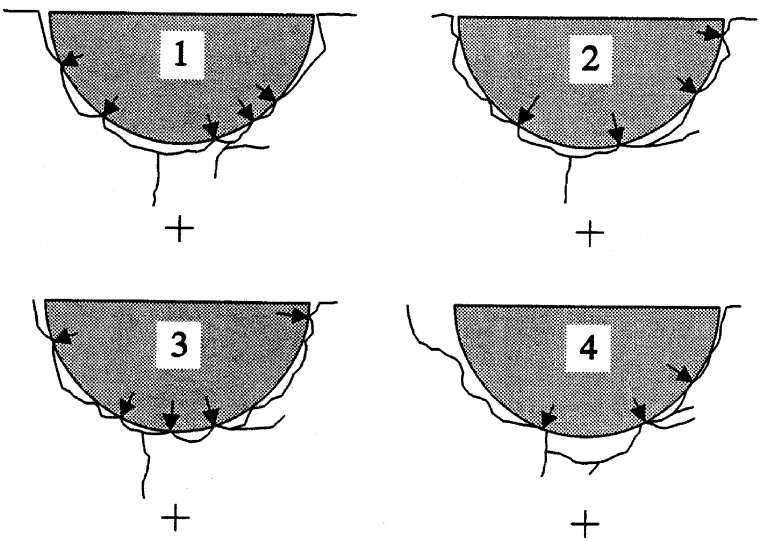

Fig. 5. Nonsimultaneous failure illustrated by tests on brittle wax, based on Ashby et al. [23].

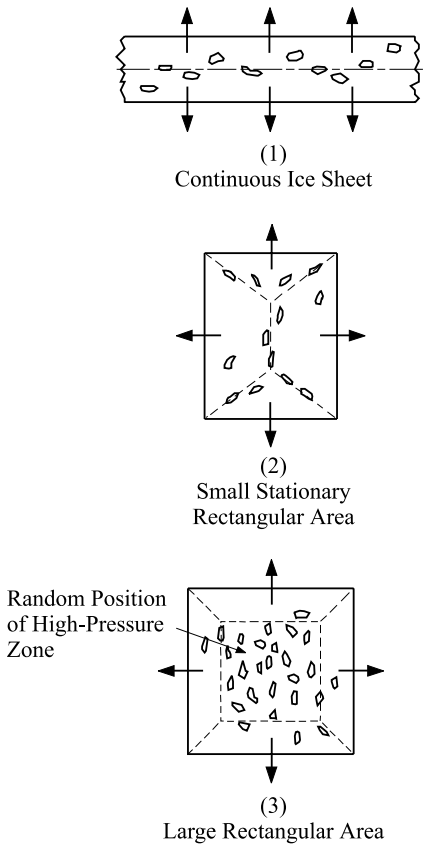

Fig. 6. Suggested arrays of high-pressure zones for various geometries. Dotted lines indicate areas where high-pressure zones tend to be concentrated [4].

For purposes of analysis and design load estimation, three areas of pressure are distinguished [1,15]. These are parts of the *nominal interaction area*, defined as the projection of the structure onto the original shape (without spalls) of the ice feature. The three areas are then the spalled area, of zero pressure for edge spalls; the area across which crushed ice extrudes, of moderate pressure; and finally the high-pressure zones themselves. Fig. 8 illustrates the idea for an area that might represent an interaction with an iceberg. The zones through which extruding ice passes will include crushed ice from the high-pressure zones, and fragments from the internal spalls mentioned in the preceding paragraph. These might break up further as they pass through this zone. In the extrusion tests summarized in Singh et al. [29], we estimated the pressure at the boundary between the extrusion and high-pressure zones to be in the range 5–10 MPa. The pressures are likely to be less than these values for extrusion in wide spaces or near the edge.

A probabilistic model of high-pressure zones has been developed based on the idealization of the high-pressure zones as point loads, as illustrated in Fig. 9 (Jordaan et al. [30], Johnston et al. [31] and Zou [32]). For the analysis, a spatial Poisson process was used to model the random number of point loads on a design area, with the size of each load being random as well. This has been compared to the extensive analysis of full scale data on ship rams, noted above. Good agreement (in the statistical sense) with measured local pressures was found. Extensions of this analysis to take into account correlations in position and size of the "point loads" is being considered.

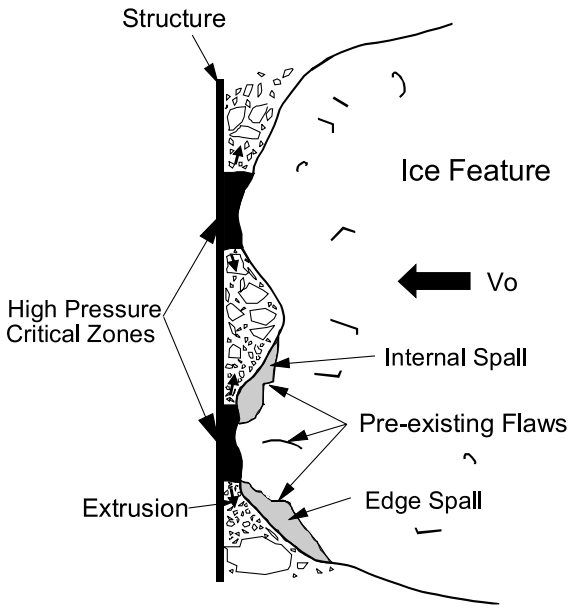

Fig. 7. Wide interaction area, showing possible "internal spall".

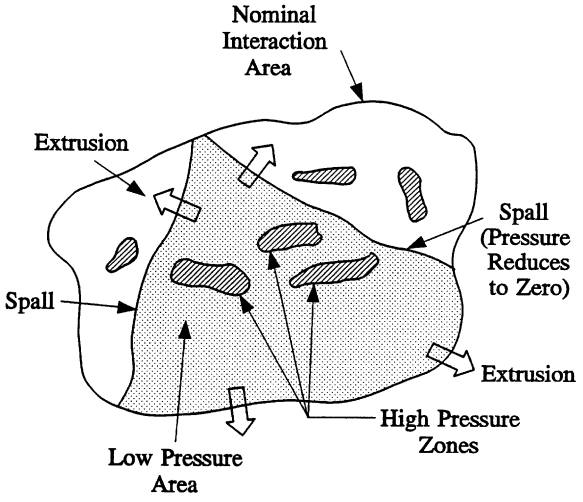

Fig. 8. Nominal interaction area and contributing components. The low pressure area contributes to the actual contact area.

4. Compressive failure: high-pressure zones

4.1. Medium scale and extrusion tests

Medium scale tests provide a good way to study compressive failure, since detailed pressure measurements and characterization of the ice after the tests are possible. Several series of these tests have been conducted. The first was conducted by the Hibernia Joint Venture Participants (with Mobil Oil Canada as

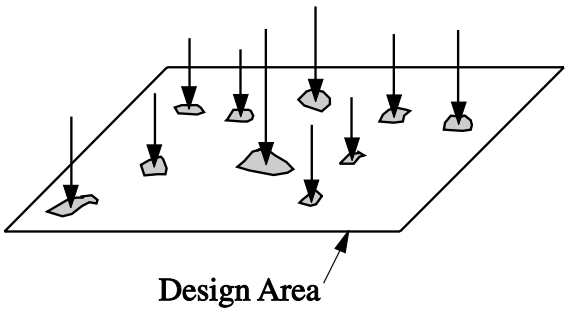

Fig. 9. Random forces in random positions for probabilistic analysis.

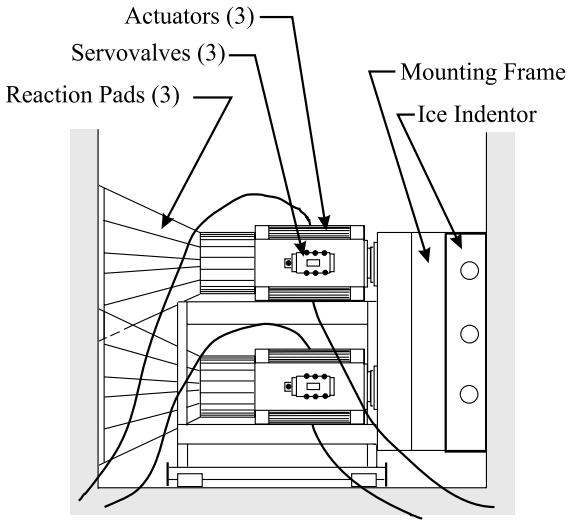

Fig. 10. Test arrangement in medium scale tests.

the operator), who commissioned the apparatus. This series was conducted at Pond Inlet in 1984 in tunnels made in a grounded iceberg and reported by Masterson et al. [33]. A second series was carried out during the winter of 1984–1985 [12]. The apparatus was then donated by Mobil Oil Canada to Memorial University of Newfoundland, and two series of tests at Hobson's Choice Ice Island [3,34] were conducted in 1989 and 1990. The experimental set-up used in the second of these is shown in Fig. 10.

Consider first the results for a slow test (#1 in the 1989 Hobson's choice series) at 0.3 mm s^{-1}. The load increased monotonically with time over a period of 90 s. The principal features of the ice deformation are shown in Fig. 11. A permanent depression with evidence of substantial damage in the vicinity of the indentor was observed. Neither ejection of ice nor localized spalling were observed. A large spall crack resulted in an ice piece 20 m in horizontal extent (Fig. 11). The damaged zone noted was found in thin sections to be significantly recrystallized into small crystals but there was no distinct layer.

For faster indentation, cyclic force-time behaviour, with layer development and extrusion of small particles, occurs. The layer of extruding ice has been shown, in the medium scale tests, to be associated with this dynamic activity. With regard to the indentor speed, it is important to consider the structural response when analysing results in the laboratory and in the field. Since the ice load fluctuates, the structure or

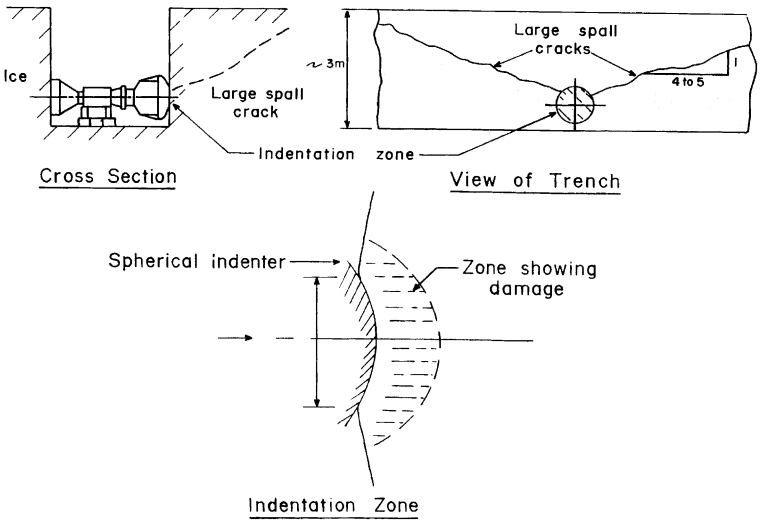

Fig. 11. Schematic of slow test results (test NRC 01).

indentor will generally respond with movements of its own; in the case of the medium scale tests, the servo-control valve could not control the rapid movements forward upon pulverization of the ice, and there was a surge forward during the unloading part of the cycle. Fig. 12 illustrates the actual displacement at the ice–structure interface, as against the nominal displacement. Three cases can be distinguished. If the indentor is very flexible (often in small-scale laboratory tests), there can be a very small relative movement on the upswing in load; the flexible indentor merely bends back. Upon extrusion the indentor moves rapidly forward, constituting most of the forward movement. (The rate of interaction will also have some bearing on this aspect.) There is essentially an energy flow into and out of the indentor [35]. For stiffer indentors (as in Ref. [35]), we calculated roughly 25–40% of the energy consumed per cycle flows into and out of the indentor (assumed to be elastic).

In the medium scale tests, the average rate of movement on the upswing in load (calculated from displacement measurements) is about half the nominal rate, since the servo-control device attempts to

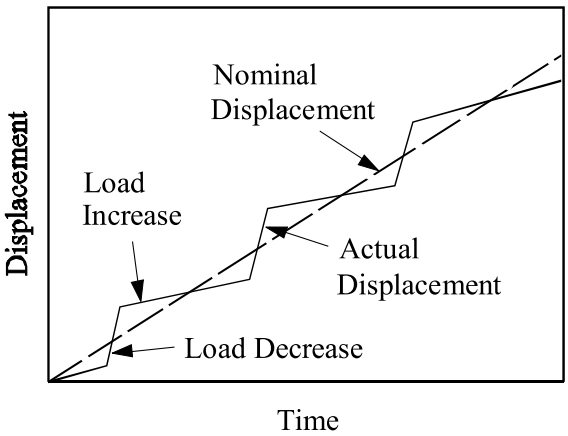

Fig. 12. Idealization of nominal and actual displacements taking into account indentor or structure response.

maintain the correct average rate, and slows down after the surge forward noted above. Detailed calculations indicate that roughly 50% of the energy per cycle is transferred to the ice on the upswing and again 50% on the downswing. This means that the power is much higher on the downswing when there is a rapid surge forward. Certainly this wide variation does not occur in the case of the Molikpaq; based on the stiffness quoted by Jefferies and Wright [2], the structure would only move about a centimetre (no plastic deformation of the foundation taken into account) while the ice is moving at many cm s^{-1} (up to 20 during dynamic events). For a load cycle lasting one second, the structural deformation is a relatively small proportion of this movement. A last point should be made on the question of the deformation of the damaged layer in the medium scale tests: even for soft layers, the resulting indentor movement is small [36], since the layer is thin.

Several examples of the appearance of the ice surface after indentation are shown in Fig. 13. The first, (a) is from the large (3 m^2) Pond Inlet test. The main feature is the extensive white layer of crushed material, with the occasional "blue zone". Kennedy et al. [37] reported on digitized sections of the layers from chainsaw cuts. The areas in which a layer was not apparent was relatively minor in these tests. In the absence of a layer, generally near a blue zone, the question arises: is the ice damaged? The second illustration, (b) is from a smaller indentor test at a rate of 90 m s^{-1}. Spalls and damaged ice with extensive microfracturing are in evidence in the outer areas, with a bluish interior. The thin sections show recrystallized material in the blue

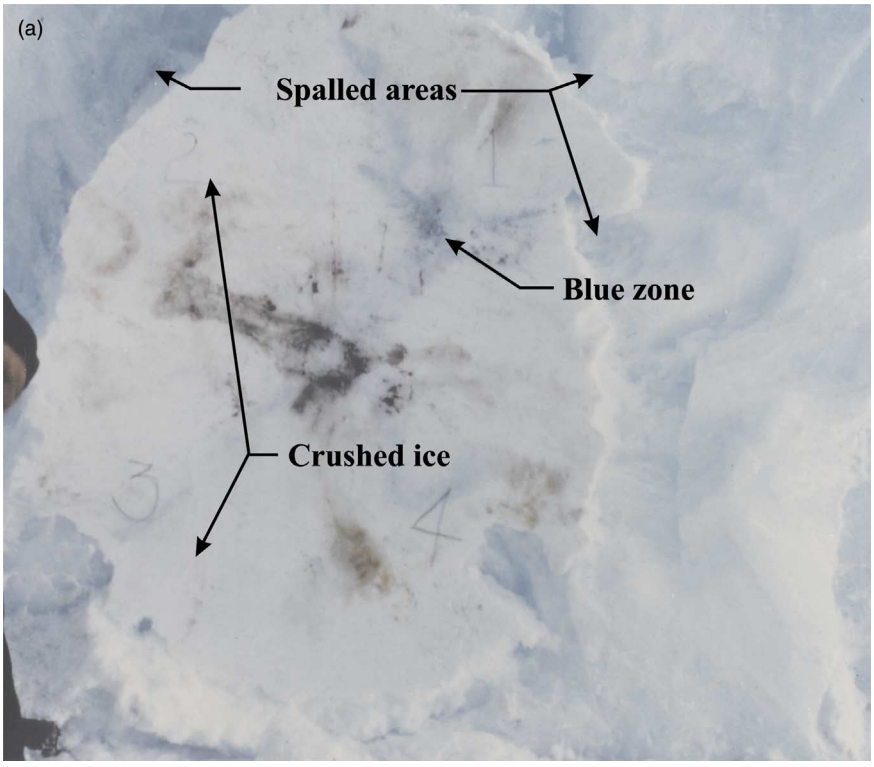

Fig. 13. Appearance of indentor surface after tests (70–100 mm s^{-1}); crushed layers, thick and thin sections: (a) Pond Inlet 3 m^2 test 1, tunnel 5, (b) Hobson's choice 1989, test NRC 05. Marks (arrows in upper right photograph) were made by Bob Frederking to show slip during extrusion (20–50 mm). Note extensive recrystallization in blue zone, (c) Hobson's choice 1989 test NRC 07. Recrystallization in blue zone less extensive than in (b) and (c), (d) Hobson's choice 1990, test TFF-01. Note extensive recrystallization in blue zone.

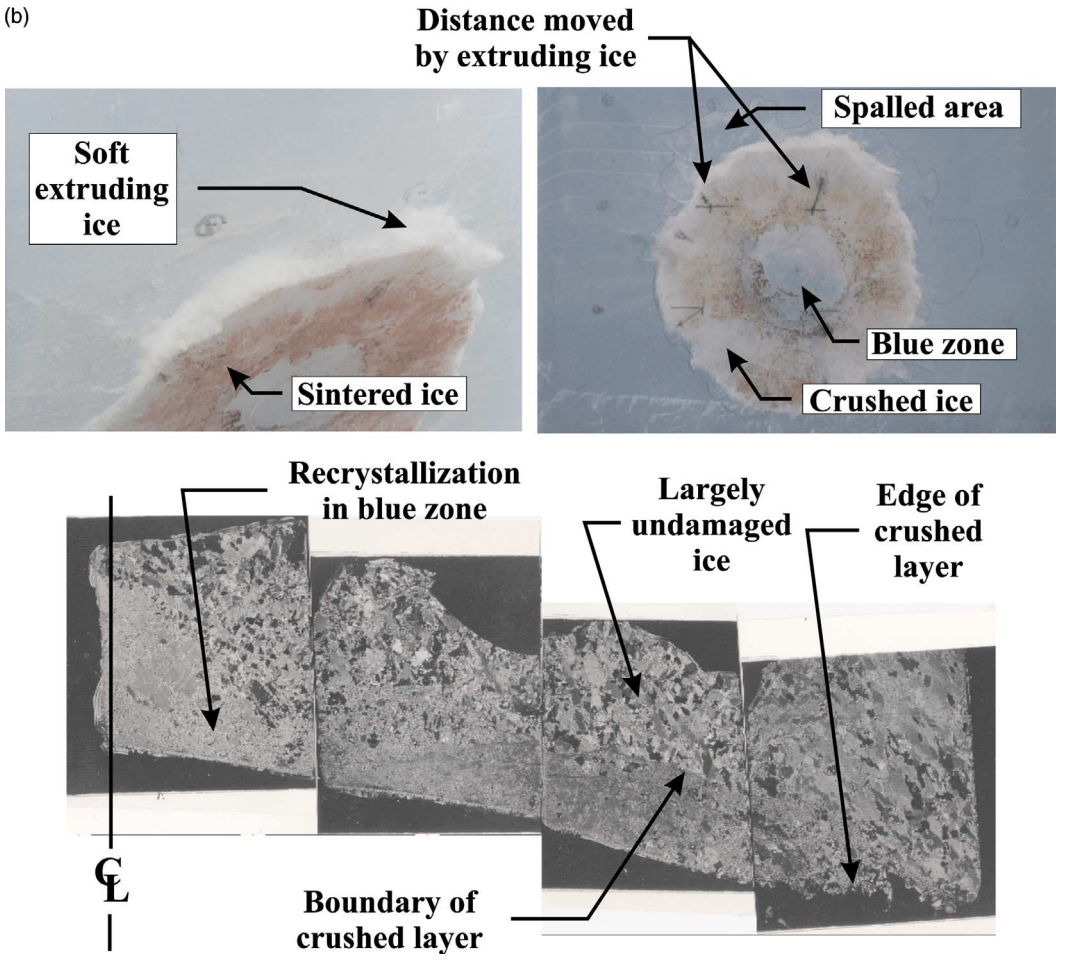

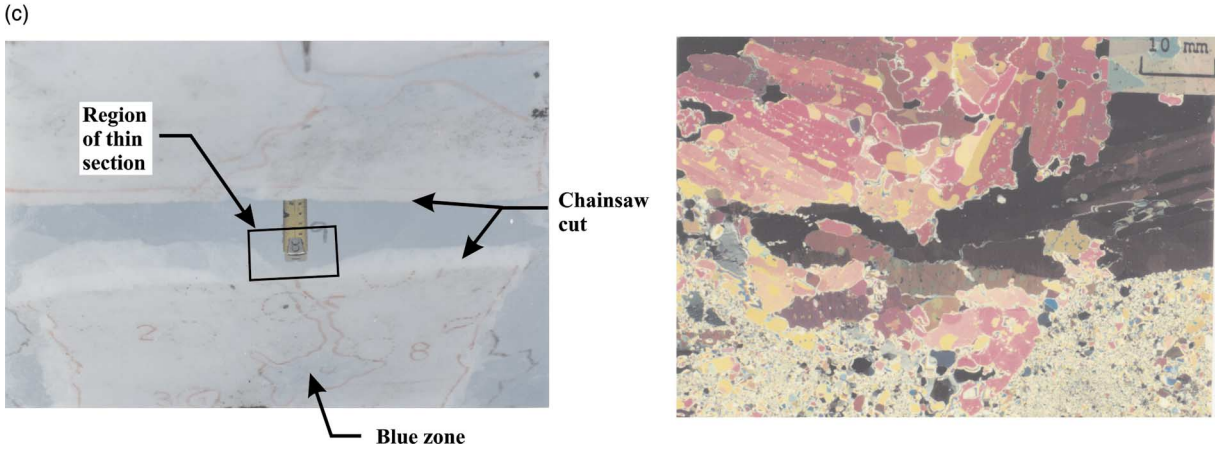

Fig. 13 (*continued*)

(d)

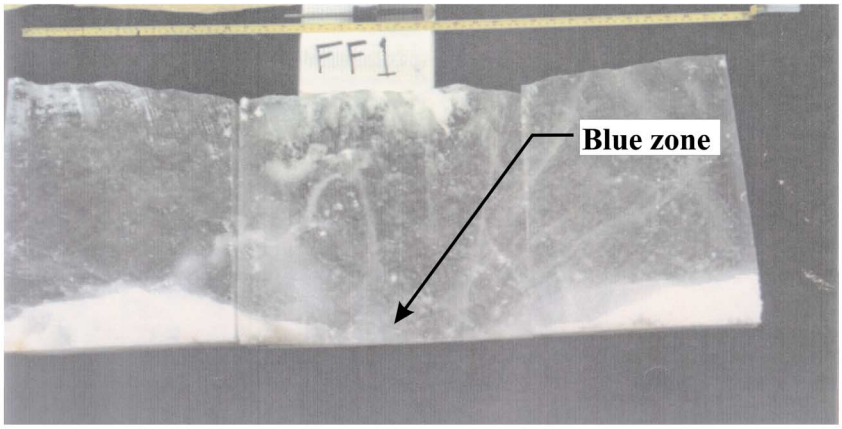

Horizontal thick sections taken from the central region of the ice-indentor interface

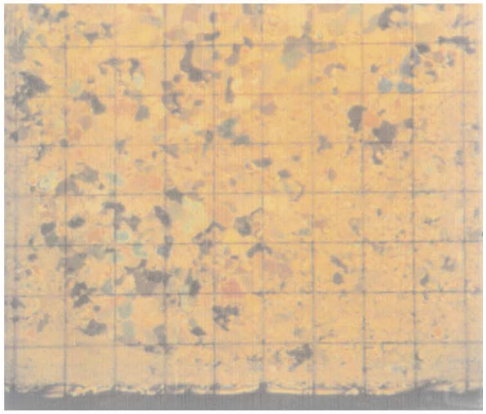

Central region of indentor face (blue zone from above)

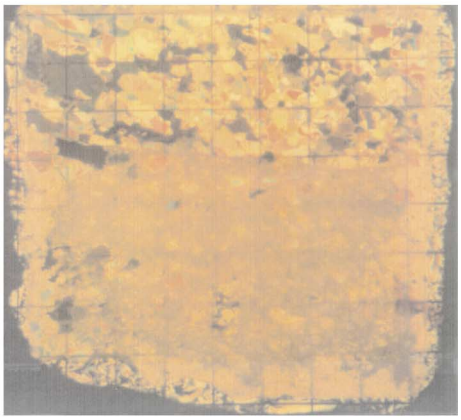

Right side of indentor face (from above)

Fig. 13 (*continued*)

zone. Fig. 13(c) and (d) shows some results from the 1989 and 1990 Hobson's choice tests. In both cases, blue zones are in evidence. The material in the layer is again highly recrystallized, as are the blue zones, rather less so in the case of (c). With regard to the 1989 series, Sinha and Cai [38] state that "The so-called 'blue' zone is not necessarily undamaged ice. Severe grain modification, primarily recrystallization, is the major feature of these zones and can reach depths of more than 100 mm". In Ref. [39] further information is found for the 1990 test series. The recrystallization noted is the "signature" of prior stress history of high volumetric stresses accompanied by shear; see Section 4.3.

The layer thickness has been seen to vary, and near the centre may be merely a damaged zone, without a distinct boundary. This corresponds in our view to the centre of extrusion, where the lateral deformation contributing to the extrusion is minimal. The velocity of extrusion, and associated strains vary from a negligible amount at the centre of the high-pressure zone to a maximum at the edge. The extrusion channel varies in thickness, with some parts wide enough to afford Mohr–Coulomb granular flow at low pressures,

extruding the crushed products of the high-pressure zone. The layer would be expected to be less developed near the centre of extrusion, where there is a "stagnation point." The blue colour that is evident where there is no extrusion channel, and would correspond (as noted) to the proximity of the centre of last extrusion, and probably near the area of highest pressure in the last cycle. These zones are often, but not always extensively recrystallized, but there is always some recrystallization. It is noteworthy that recrystallization is time dependent, with an initial period of breakdown of structure (discussed in the next section). It is believed that high-pressure zones can form on the sintered layer and that the blue area is not always present, as borne out in the extrusion tests on crushed ice [29].

The force and pressure-time curves obtained in the medium scale tests show considerable regularity in terms of the time-dependent variations. Fig. 14 shows typical results for force and pressure, the latter within the central area of indentation. Fig. 15 shows a phase-plane diagram of the kind used to depict a narrow-band stochastic process [40]. Spectral densities also show a concentration of frequency content in a narrow range. It is seen from the information just discussed that the compressive ice failure process is extremely regular; on occasion, the cycles repeat themselves almost exactly. The regularity may be interrupted by spalls, as shown in Fig. 14.

4.1.1. Extrusion tests

The extrusion tests [29,41] (Fig. 16) provide important information on layer behaviour. In these, crushed ice particles were squeezed between two rectangular plates (762×508 mm, with extrusion constrained to occur in the "long" direction) at various speeds. The gap between the plates was initially about 100 mm, which reduced to a few centimetres at the end of the test. Mohr–Coulomb flow with the pressure distribution appearing characteristically as a convex function curving upwards from the edges at the lower pressures, and a concave function of distance at the higher pressures (Fig. 20). The latter indicated a transition to pressure-independent viscous flow (albeit highly nonlinear), and sintering of the ice particles. This behaviour is illustrated in Fig. 16; there was also regular sawtooth variation of force and pressure. No spalls were possible because of the geometry. The behaviour can be explained by the present theory, but not on the basis of spalls and fractures.

4.2. Discussion: layer formation

The results indicate first the transition from ductile to brittle behaviour in specimens of ice, as the loading rate is increased [42,43]. Triaxial stress states with varying confinement develop within the high-pressure zones and the transition from ductile to brittle behaviour becomes a complex function of these states. For periods of time, ductile behaviour can exist within the high-pressure zones adjacent to the structure with brittle failures in the "hinterland." Brittle behaviour is found in the medium scale at rates higher than a few millimetres per second. At rates above 3 mm s^{-1} [12], the load becomes cyclic in nature and large amounts of crushed ice are produced. This is seen also in ice–structure interaction such as the "Molikpaq" events mentioned, and crushed ice particles are seen in ship–ice impacts, in ice–ice interaction, and was (as noted) found in the medium scale tests.

Fig. 17 summarizes schematically the behaviour of a high-pressure zone during the cycling of load. This is the best estimate of the writer at the present time; no doubt, details will be clarified or corrected as further knowledge is obtained. Fig. 17 is based on a similar figure in Jordaan and Singh [44], but has been drawn to illustrate the behaviour if the ice in the contact area is not significantly damaged prior to the load cycle. Damage first forms near the edge of a high-pressure zone. Nucleation of microcracks occurs across the basal planes, at points of stress concentration, with extensive recrystallization. This results in extensive microfracturing near the edges, with the formation of a white zone containing cracks and air pockets. Recrystallization occurs along with the microfracturing. The growth of microcracks results in coalescence and finally fragmentation of the material near the edges of the zone. The centre of the high-pressure zone

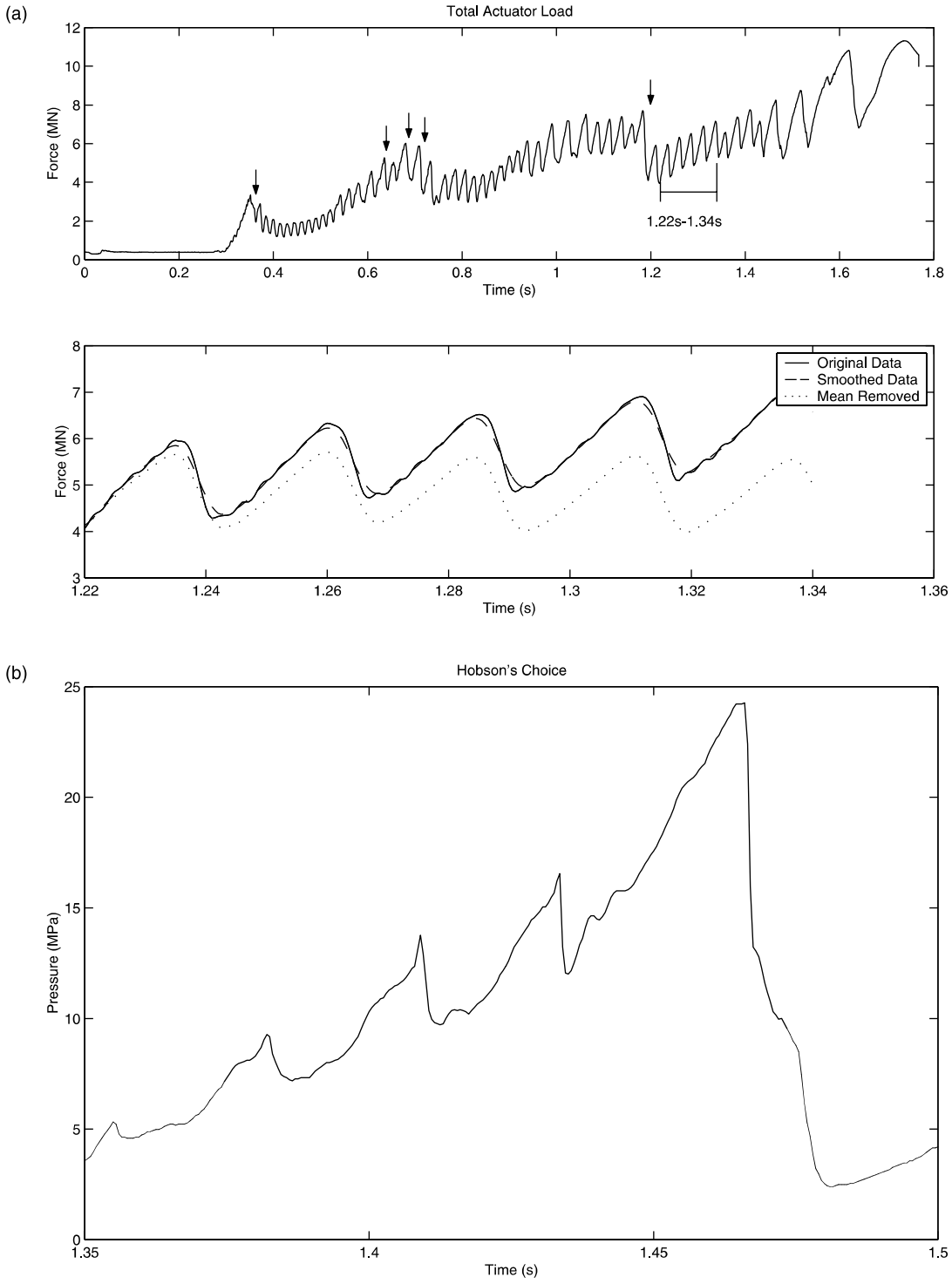

Fig. 14. Measured regular sawtooth variation of load in medium scale tests is shown in (a); pressure shown in (b); often there is an increase in pressure near the peak load, as also suggested in Fig. 17. Possible spalls shown by arrows.

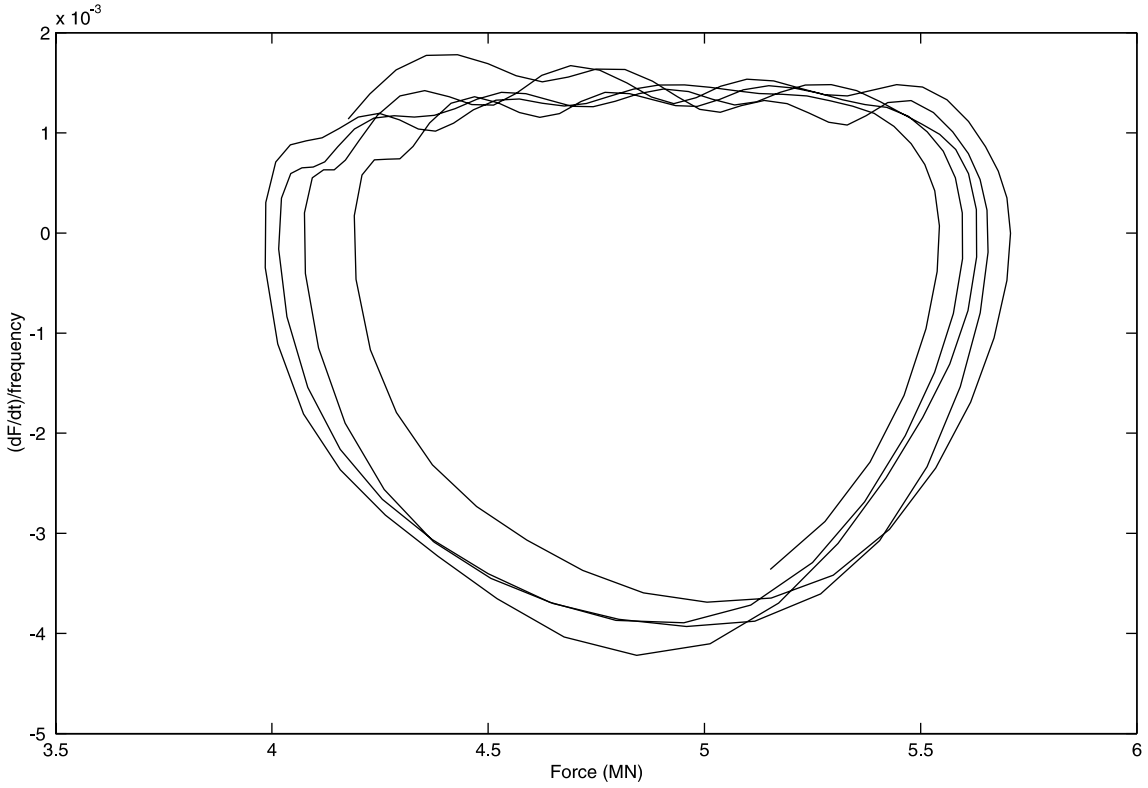

Fig. 15. Force against normalized rate of change of force (phase-plane diagram), showing regularity over several cycles, for period 1.22–1.34 s in Fig. 14.

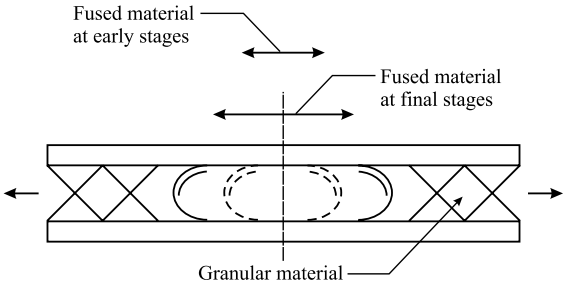

Fig. 16. Schematic of extrusion tests (vertical scale exaggerated). Variation of lateral dimension of fused material along extrusion axis [29]; "early stages" means just after load drop; "final stages" means just before load drop.

exhibits pressure softening [45–47]. This is manifested in the recrystallization process at high pressures, resulting in fine-grained material. This is discussed further in the next section. In the cyclic behaviour, the pressure softening process which occurs towards the peak load, reverses itself when the pressure drops.

Slip at both boundaries of the extrusion channel is in evidence. The marks on the ice-indentor interface in Fig. 13(b) indicate the distance moved by the ice relative to the indentor. As part of the present programme, a set of tests [48–50] has been reported. In the third of these [50], thin sections from an actual interaction of a small iceberg with a structure were made. One result is shown in Fig. 18, in which clear

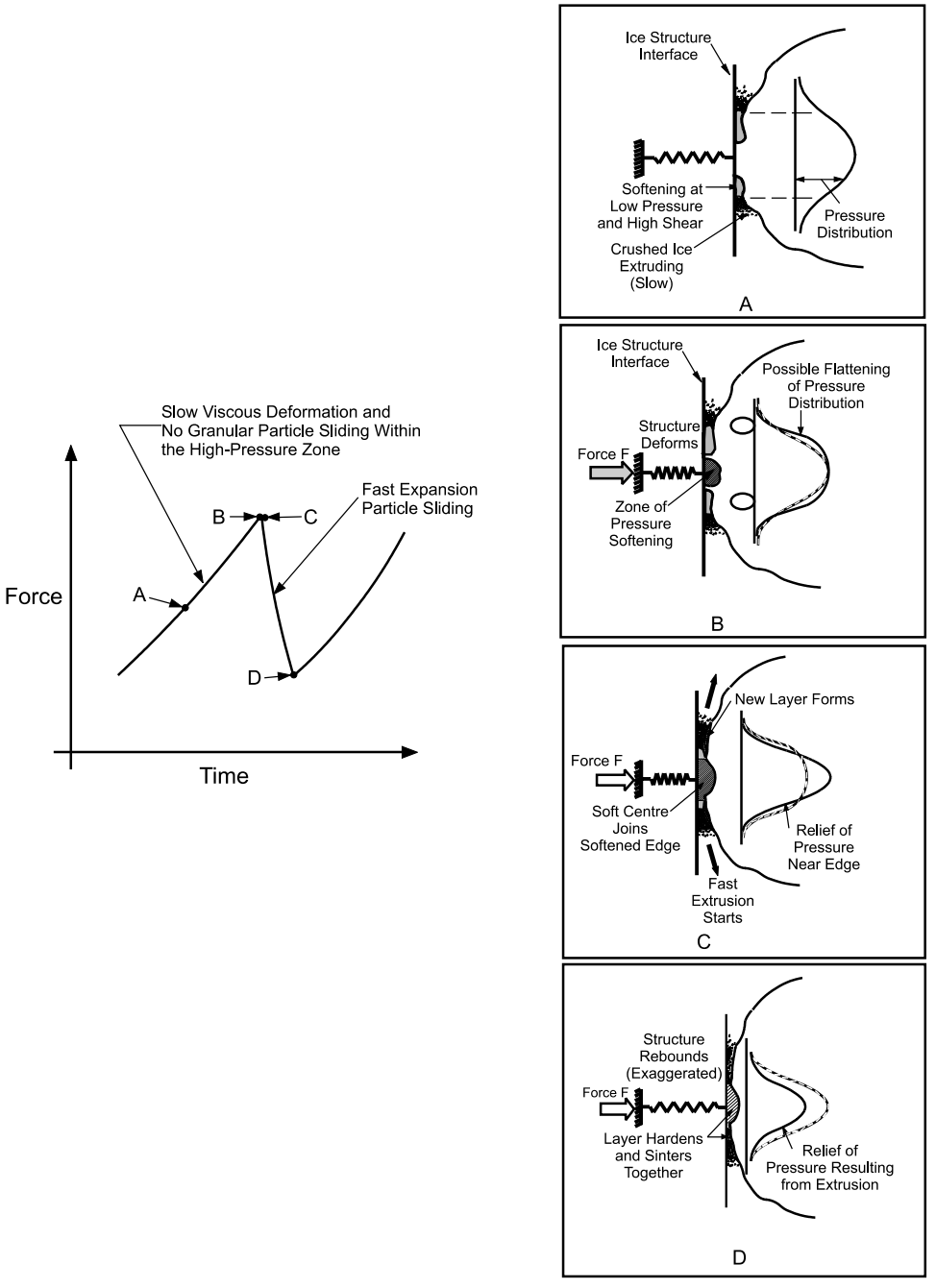

Fig. 17. Schematic summarizing the load fluctuation and associated processes in a high-pressure zone. The ice will generally be damaged at the outset. The failure process is unique; a high-pressure zone will have distinct failure load.

evidence of slip along the edge of the damaged layer is evident. We refer also to Fig. 19, in which the effect of slip on the shear and velocity profile within the softened layer is illustrated. It seems likely that slip

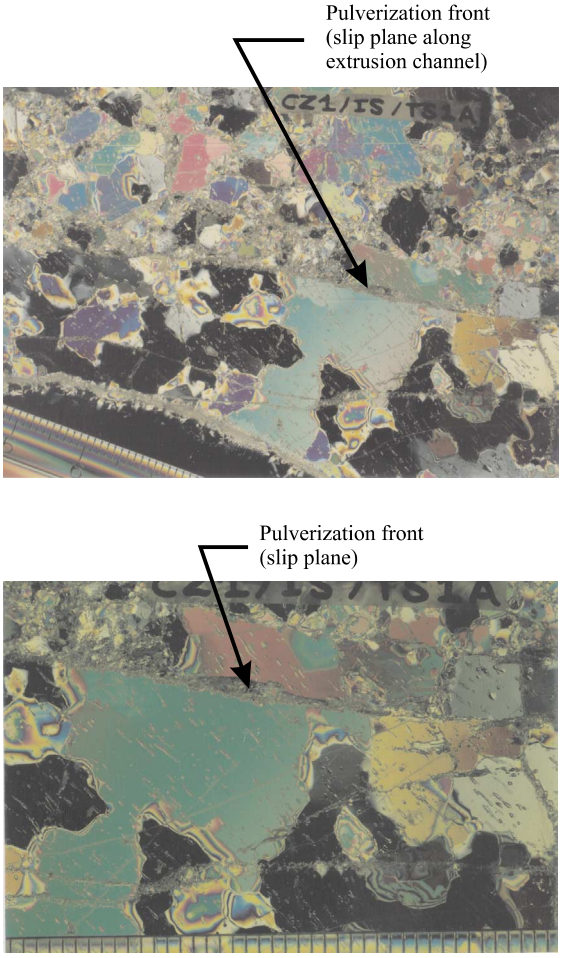

Fig. 18. Thin section of extrusion along pulverization front in Grappling Island tests on iceberg impacts [50].

commences at or near the peak load, when the mismatch between the damaged layer and the virgin ice causes large shearing stresses. Outside of the high-pressure zones, in the wider spaces of extrusion of crushed ice, slip may take place continuously.

A most striking and incisive analysis was provided by Kheisin and his co-workers (Kheisin and Cherepanov [46]; Kurdyumov and Kheisin [51]). In 1967, they performed dropped ball tests with a steel ball weighing 300 kg. They examined the microstructure before and after impact. Velocities were in the range 1–6 $m\,s^{-1}$, much higher than in the medium scale tests discussed below. They were the first, in the author's knowledge, to draw attention to the fine-grained nature of the ice in the layer, which appeared to cover the entire contact zone. They pointed out that the process produces "lamellae up to 0.5 mm thick, formed by shear over the basal planes" which were then broken up into "small roughly-cubical crystals". They also pointed to the existence of ice particles of submicroscopic size dispersed amidst these crystals and acting as a "lubricant for the matrix", resulting in a "finely dispersed crushed layer behaving as a layer of viscous liquid". Attention was also drawn to the effect of pressure melting and frictional heating. Kheisin's work also led to the analysis of extrusion, treating the crushed layer as a viscous fluid, using essentially lubrication theory.

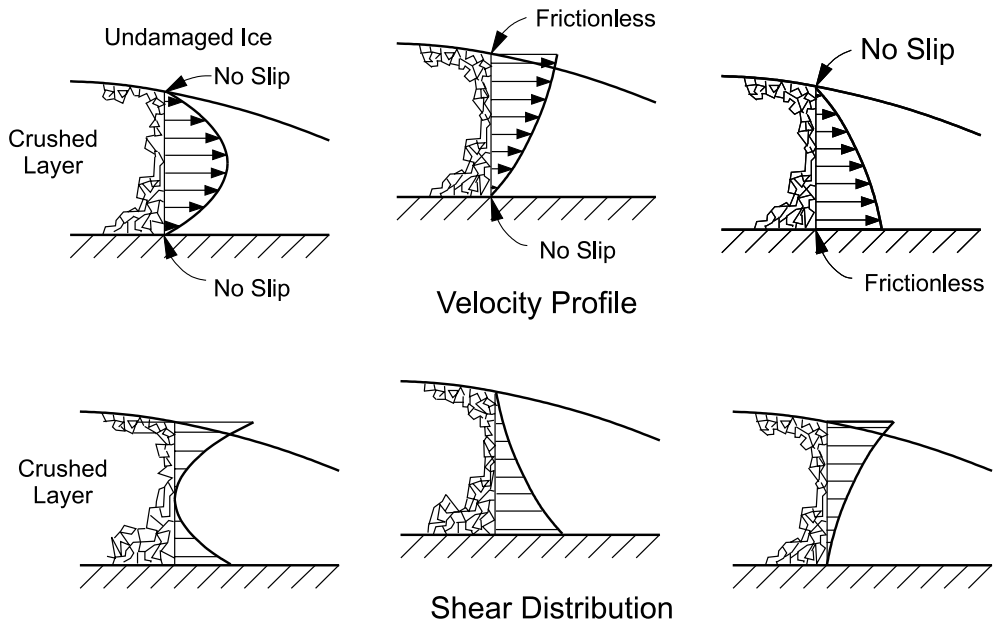

Fig. 19. Illustration of slip developing at the upper and lower surfaces of the damaged layer, and associated changes in shear and velocity profiles in a viscous layer. Top and bottom sketches correspond.

As a result of medium scale tests, extrusion tests and other observations discussed above, it was concluded that the ice sintered together after each load drop [1]; particles did not slide over each other – in the sense of granular flow – within the high-pressure zones on the upswing in load; rather, there was soft viscous flow, corresponding to the response of damaged ice. It is certain that granular flow did occur outside these zones in large-scale interactions such as the Molikpaq events, in the clearing process. Further, the pulverization of the high-pressure zones was found to consist of movements parallel to the structure interface of the boundary between the sintered ice and the granular ice (Fig. 16). High-pressures zones were seen as the ''staging post'' between practical analysis and more fundamental studies [52].

To introduce the next section, it is most important to understand the *nonuniformity of the compliance of high-pressure zones*. Let the short term compliance including creep of undamaged ''virgin'' ice be unity. Damaged ice, or ice that was previously damaged but is now sintered, may have a compliance that is 100 times the virgin value or more. This does not mean that there will be particles sliding over each other within the high-pressure zone (as in extrusion) on the upswing in load, but rather greatly enhanced creep deformation. The material under sufficient confinement remains quite transparent, although much more fine grained. The third kind of deformation, consists of the granular flow of crushed ice, near the edges of the high-pressure zones and in the wider spaces between them (see Fig. 7); this flow is more compliant again than the sintered or damaged ice. It is Mohr–Coulomb granular flow; for analysis using rate-independent theory, see Duthinh [53]. The transition from viscous processes is illustrated in Fig. 20 [1]. Fig. 19 shows the effect of slip (particle sliding) along the boundaries on the velocity and shear in a viscous layer. The behaviour would be predominantly viscous on the upswing and involve more granular flow on the downswing of Fig. 17 [54]. It appears that slip develops at the boundary of the pulverization front at the peak load, as a result of the mismatch in compliances. The failure process of a high-pressure zone is unique, with a distinct failure load.

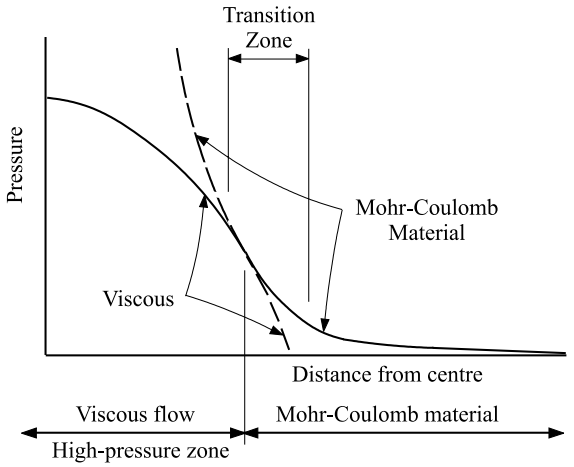

Fig. 20. Transition from viscous behaviour to Mohr–Coulomb flow near the edge of a high-pressure zone. The point of transition moves inward upon zone failure.

4.3. Detailed mechanics of high-pressure zones: triaxial tests and damage process

A programme of work was instituted to formulate models of the failure process in the high-pressure zones in some detail [48–50,52]. This comprised a linked programme of triaxial testing of ice under compressive states, and associated constitutive modelling. The results were incorporated in finite element modelling [52] of the failure process within high-pressure zones. Fig. 21 shows the purpose of the triaxial testing. This was to determine the behaviour of ice under stress states that might be found in the zones. The programme included study of the stress–strain behaviour, linked to the underlying damage and microstructural processes. For the most part, the ice was polycrystalline and granular, grown in the laboratory [48,55]. Tests have also been performed on crushed ice with associated constitutive modelling [56]. These were conducted under triaxial states of stress, with the confining pressure being applied first. Both creep (constant-stress) tests and constant strain-rate tests were done. The calibration was based mainly on the constant-stress tests.

The results of the tests on polycrystalline ice are typified by Fig. 22, as regards changes to microstructure at low and high pressures. The pictures represent the structure at 4% and 44% strain under constant stress states. It can be seen that very realistic representations of the process in a high-pressure zone are obtained, compared to the results given in Fig. 13. Microfracturing of the ice is in strong evidence at the lower pressures, and much less so at high confining pressures. The ice in both cases has been highly recrystallized. The recrystallization occurs along with microfracturing at lower pressures, and with little cracking at high pressures. The mechanism appears to be different in some respects from the recrystallization that occurs during the formation of subgrain boundaries (dislocation walls) during deformation. Strain rates of the microstructurally modified material are much enhanced; see Refs. [57,58] for uniaxial conditions. The increase in creep rate in the early tests under uniaxial stresses at low strains was not sufficient to explain the behaviour of the crushed layer, as outlined in the discussion of the finite element analysis below. The changed compliance can be expressed as a function of appropriate state variables representing the crack density; see Ref. [59] for the elastic case. A key point turned out to be the application of the high stress levels and triaxial stresses, as in Refs. [48,49]. It became clear during the research programme described that the behaviour of high-pressure zones involved a much wider range of processes, including recrystallization, microfracturing, crack healing, and pressure softening. The compliance of the ice with altered

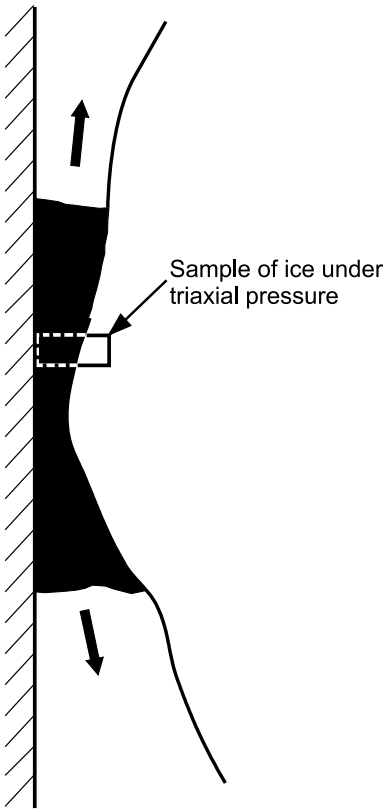

Fig. 21. Purpose of triaxial tests; to study damage process in states of stress representative of that in actual high-pressure zones.

microstructures such as those illustrated in Fig. 22 was found in some cases to result in strain rates of the order of 100 times or greater than that of undamaged ice.

The stress–strain response was modelled using damage mechanics [52,60], using necessarily a somewhat simplified approach. The strains were divided into elastic, delayed elastic and flow terms [61]. Two approaches were taken, first, based on an analysis of viscoelasticity using springs and (nonlinear) dashpots, and second, based on Schapery's correspondence principles [52,56,57,62]. It was found that the flow term predominated for highly damaged ice. The strains are highly nonlinear, and we summarize briefly the modelling based on the analogy between elastic and viscoelastic problems. The modelling of damage was much influenced by the work of Schapery [62]. For the elastic solution, the following stress potential was used.

$$W^c = \frac{\varepsilon_0 \sigma_0}{n+1} \left(\frac{s}{\sigma_0} \right)^{n+1}, \tag{6}$$

where ε_0 and σ_0 are constants, n defines the nonlinearity, and s is the von Mises stress defined as

$$s = \left(\tfrac{3}{2} s_{ij} s_{ij}\right)^{1/2}, \tag{7}$$

where s_{ij} is the deviatoric stress; the von Mises strain is defined analogously. The deviatoric strain e_{ij} is given by $e_{ij} = \partial W^c / \partial s_{ij}$, and the strain rate for the flow term follows by analogy, i.e. strain rate replaces strain. The approach can be extended to consideration of volumetric effects and the presence of voids [56,63]. These effects will not be discussed further here.

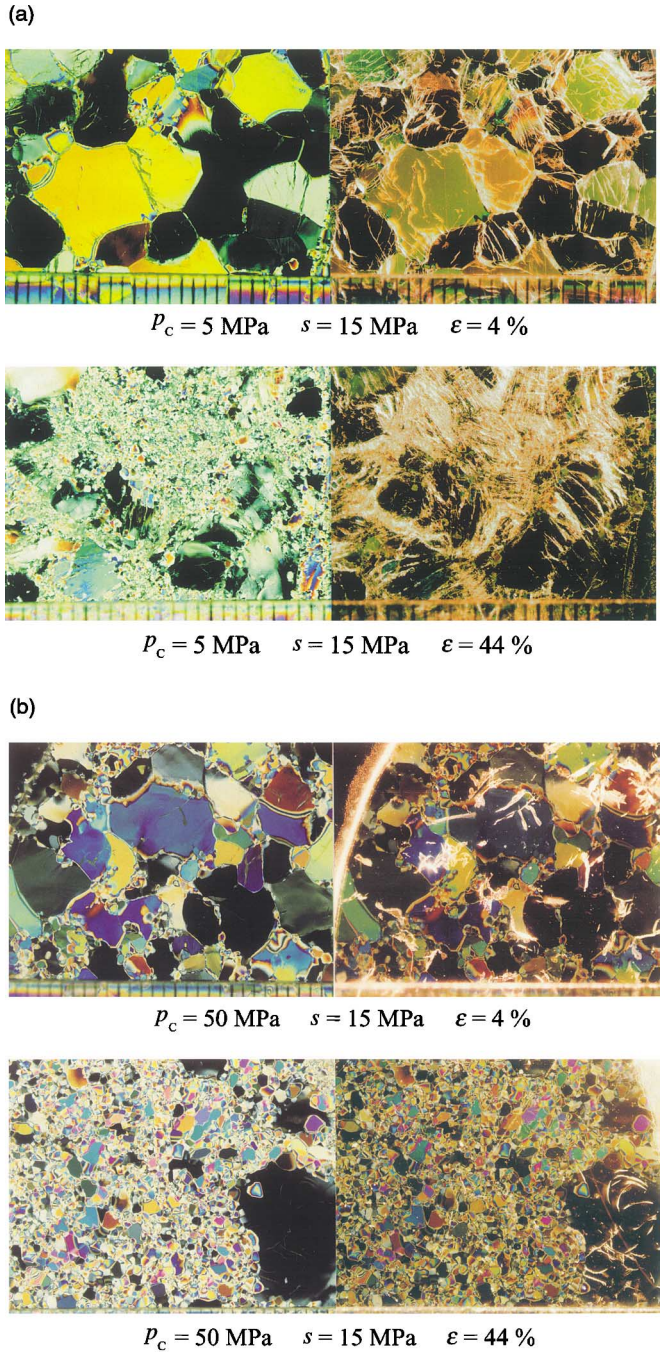

Fig. 22. Thin sections through crossed polarizing filters (left) and crossed polarizing filters with side lighting (right); (a) $p_c = 5$ MPa, $s = 15$ MPa, $\epsilon = 4\%$ (top), 44% (bottom); (b) $p_c = 55$ MPa, $s = 15$ MPa, $\epsilon = 4\%$ (top), 44% (bottom). Note that $p_c =$ confining pressure, $s =$ deviatoric stress, $\epsilon =$ axial strain. Results from Meglis et al. [49].

The resulting flow may be interpreted in terms of an apparent viscosity μ:

$$\mu \propto g^{-1}(S_{\sigma 1}, S_{\sigma 2}) s^{-(n-1)}, \tag{8}$$

where $g^{-1}(S_{\sigma 1},S_{\sigma 2})$ is the viscosity reduction factor due to the damage level $\{S_{\sigma 1},S_{\sigma 2}\}$. An exponential form of $g(S)$ was used (for background, see Refs. [52,62,64]):

$$g(S_{\sigma 1}, S_{\sigma 2}) = \exp(\beta_1 S_{\sigma 1} + \beta_2 S_{\sigma 2}), \tag{9}$$

where β_1 and β_2 are constants, and

$$S_{\sigma i} = \int_0^t f_i(p) \left(\frac{s}{s_0} \right)^{q_i} \mathrm{d}\tau, \quad i = 1, 2, \tag{10}$$

are the state variables representing damage. The results of the comparison with data are shown in Fig. 23. The results showed that the material softened at low pressures, where there is considerable microfracturing, governed in the simulation by $f_1(p)$. At higher pressures, softening associated with pressure was observed; this has been approximated by the function $f_2(p)$. It is considered that this captures the spirit of the phenomenon; see Ref. [52] for further details.

The results of the constitutive modelling were included in finite element modelling using the UMAT subroutine in the program ABAQUS. In earlier attempts, damage was modelled for lower pressures [65]. The work aimed at a spatial representation of the compliances as a function of the state variables noted. Figs. 24 and 25 give the main results [52]. The model allowed slip at the interface between the crushed layer and the structure. The four stages in Fig. 25 correspond to the points indicated in Fig. 24. It is seen that damage commences near the edges of the high-pressure zone, as observed in test results, and softening is then found near the centre, at peak load, also as observed. In later simulations performed by Xiao [66], by increasing the exponent q_2, and other modifications to the constitutive equation, steep drops in load were obtained. A friction coefficient at the interface between the ice and the structure was included in Xiao's work; the resulting simulation provided similar results to those just given. A typical linear dimension of the zone based on field observations would be 30 cm. But the analysis described does not depend on the scale, and should apply, within the limitations of the assumptions, at all scales. This opens up interesting possibilities for considering results at different scales.

It is considered that the results present a convincing explanation of the observed phenomena. On the downswing in load, the pressure melting effects would reverse themselves, crushed ice particles would tend to sinter together, the load would increase again, and the process would tend to repeat itself. This seems a

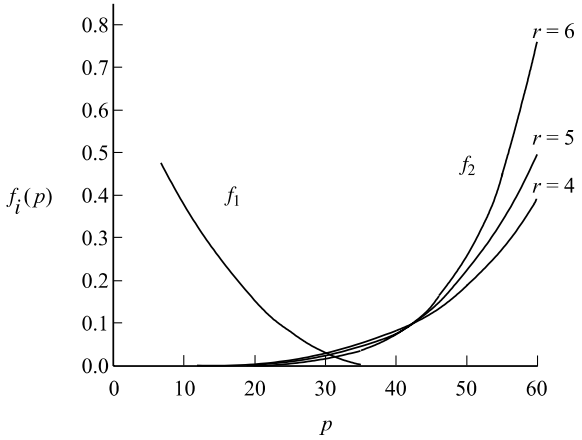

Fig. 23. Damage coefficients as a function of pressure.

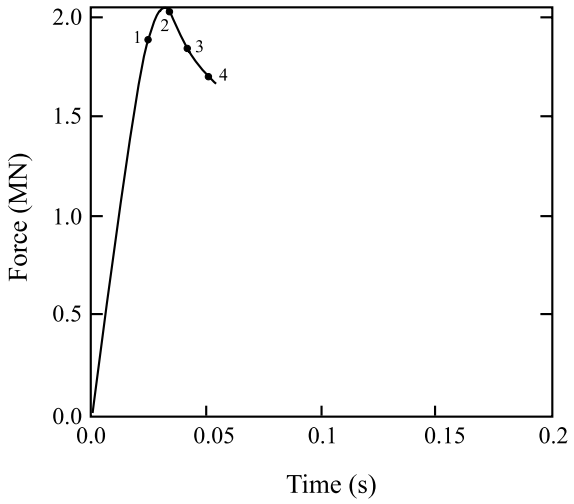

Fig. 24. Result of finite element simulation, in terms of variation of force.

reasonable explanation of the observed regularity. Failure starts at the outside, with the high gradient of shear induce by mismatch of properties, resulting finally in slip when the centre softens too. Geometry dictates that the slip increases from near zero at the centre of extrusion to the outside. Once the ice particles are granular, as slip takes place, they tend to flow according to a Mohr–Coulomb criterion [53].

Some workers resort to the use of fractals as a means of characterizing the progress of damage. These are mathematical entities that require conditions of self-similarity that are assumed. It is difficult to find demonstrations of the validity of these assumptions. The process of fracture, microcracking and damage will follow the laws of thermodynamics, as manifested in fracture mechanics, physics of surfaces and recrystallization. Mathematical devices do not necessarily contribute to an understanding of these phenomena, and often lead instead to an oversimplification of the mechanics.

4.4. Approximate (simplified) analyses

There may be need, for engineering purposes, of simplified methods of analysis. In view of the discussion of mechanics above, the idealization of Kheisin of a viscous layer is considered most appropriate. The varying thickness of the layer, for example at ''blues zones'', can be handled by varying the layer thickness, and making it thinner if desired in these zones, The work in collaboration with Maes, reported in Ref. [1], offers many solutions of this kind. This is not to say that more detailed fundamental studies should not be undertaken of the break up process; the simplification is suggested for approximate analysis. Indeed, for most purposes of design, treating the high-pressure zones as point loads, with attendant statistics, provides sufficient detail. Yet any further fundamental work that sheds light on the failure process can be used to support design information. Many insights can at the same time be obtained from Kheisin's approach, for example Fig. 19; a soft (yet solid) absorbing layer is provided by the ice to absorb energy as the indentation proceeds. There is a need to attempt nonlinear approaches to the viscosity, and, as pointed out above, the properties vary significantly along the layer.

Some workers have attempted an approximate Mohr–Coulomb slip analysis to explain the regular repetitive layer failures of Fig. 14. Fig. 26 illustrates the idea. This approach should not be confused with the rigorous Mohr–Coulomb analysis of the flow of granular materials (at lower confining pressures) noted

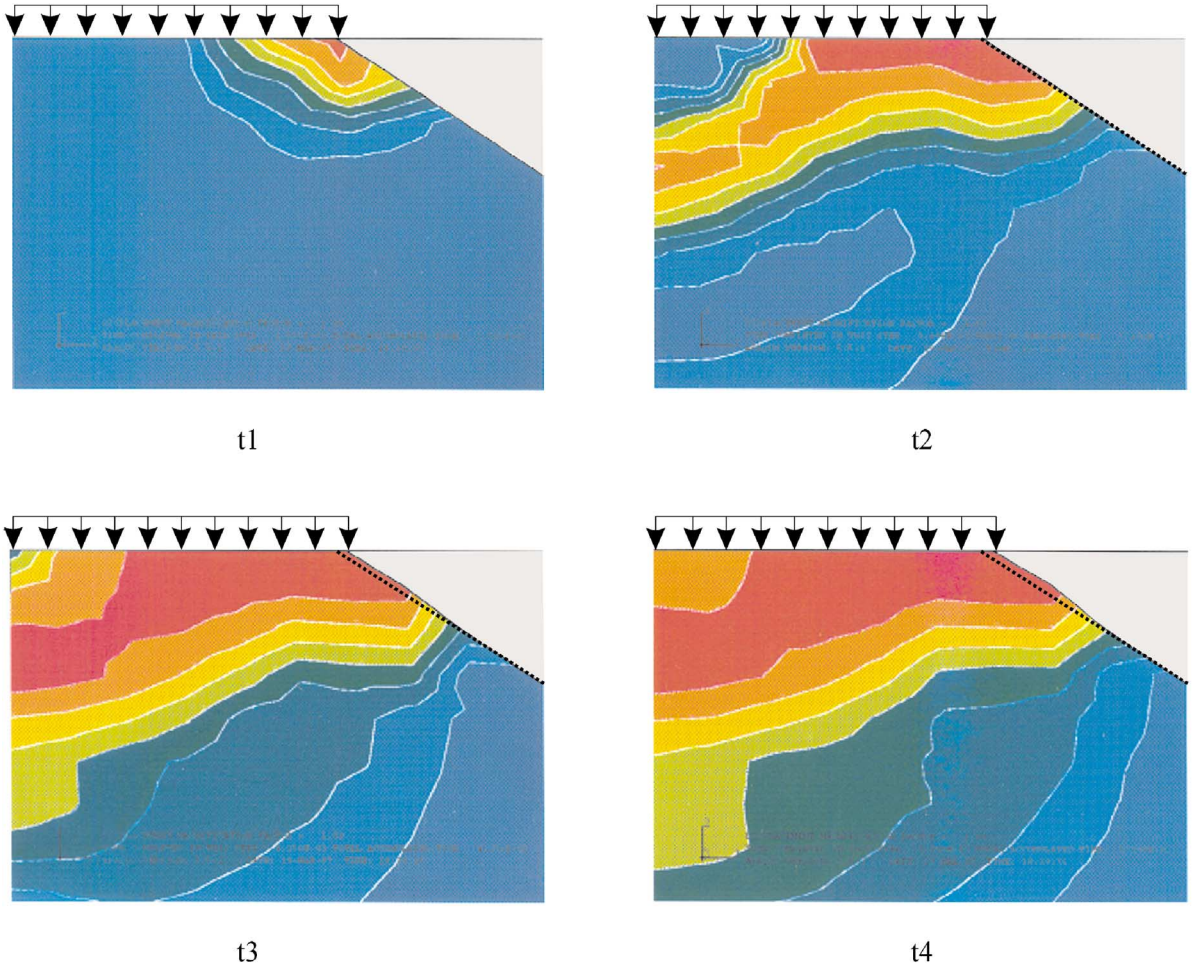

Fig. 25. Progression of damage in finite element simulation. The simulated high-pressure zone is 150 mm in diameter, with the load applied as shown, corresponding to a rigid indentor moving at 50 mm s^{-1} [52].

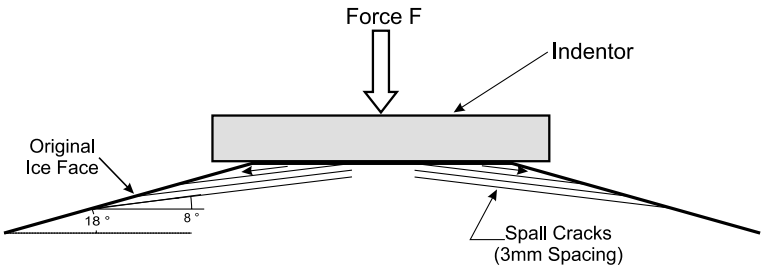

Fig. 26. Approximation of repetitive failure by Mohr–Coulomb shear planes.

above. Repeated failures across a plane are supposed in Fig. 26 to explain the cyclic behaviour, producing "sheets" to break off. Some difficulties are as follows: (1) The failure plane traverses material with varying

stress from low pressure and high shear at the outside, to higher pressure and higher shear part way to the centre, to high pressure and small shear at the centre. A single failure criterion for all of these stress states is not appropriate. (2) Singh et al. [29] suggest that the friction angle approaches zero for crushed ice under high pressure, implying pressure-independent behaviour. This does not support the Mohr–Coulomb analysis; Sammonds and Rist [67] also suggest that the Mohr–Coulomb analysis does not apply under triaxial states of stress. (3) Often the pulverization front is parallel to the structure surface, or even curved upwards, as in the case of dropped ball tests. (4) Regular failures in the medium scale occur every 2–3 mm; it is hard to visualize the failure process composed of parallel failure planes at this spacing, as in Fig. 26. (5) The process after each failure needs clarification; How do the sheets become crushed ice, with no evidence of their history? (6) What drives the crack separating the layer from the virgin ice? It appears to traverse entirely compressive states of stress.

There is a clear need to consider shear induced by the soft layer.

5. Fracture processes

It was noted in Section 1 that the formation of ice in nature is a geophysical process in which flaws, fissures and irregularities are produced. Further, the analysis of medium and full scale data exhibits a considerable scale effect, typified by a decreasing nominal pressure with contact area, as noted in Section 2. A very reasonable explanation of this effect is the occurrence of spalls and fractures as outlined in the paper. Ice is a very brittle material under high loading rates. Gold [68] and Palmer et al. [69] first recognized the importance of the extreme brittleness. Timco and Frederking [70] performed early measurements; fracture toughness values of the order of 0.10–0.14 MPa $m^{1/2}$ were reported. The resulting energy release rate (taking the elastic modulus as 10 GPa) is in the range 1–2 J m^{-2}.

Recent work by Dempsey [71] and Dempsey et al. [72] has thrown new light on the fracture process with regard to specimen size. He performed two major series of field experiments, one on warm freshwater ice with a size range of 1:81, and the second on first year sea ice. The geometric configurations were self-similar; referring first to the sea ice results, the size-independent fracture toughness was of the order of 0.25 MPa $m^{1/2}$, suggesting fracture energies four times the values just quoted. The primary reason for these results is given as the creep microcracking ahead of the crack in the "process zone". One may speculate that other processes of damage such as recrystallization may also be taking place. Work on the damage process under combined states of stress including tension are needed. In the tests on warm freshwater ice, energies up to 20 J m^{-2} were calculated, attributed to nonlocal energy absorbing mechanisms such as grain boundary sliding.

Mulmule and Dempsey [73] developed a time-dependent model, using linear viscoelastic theory. This is useful at appropriate strain rates for the material outside the process zone. The latter was treated using a cohesive zone model, termed the "fictitious" crack model. For practical analysis, a size effect relationship base on self-similar assumptions has been proposed [74], and indeed it should well be reasonable to use a constant value over certain ranges of size. We have noted in the discussion of the medium scale tests above, that time-dependent fractures occur if the loading is maintained for a long enough period. It has also been noted that ship captains cause their vessels to "lean" on the ice during ramming [4], resulting in time-dependent fractures that aid in arctic navigation. To capture the spirit of these time-dependent fractures, a crack length $2a$ was considered in Ref. [13]. The crack growth rate was modelled as

$$\dot{a} = c_1 J^k, \tag{11}$$

where J is the energy release rate, and c_1 and k are constants. This is a well-based relationship for viscoelastic materials [13,75], and the analysis leads to the following equation:

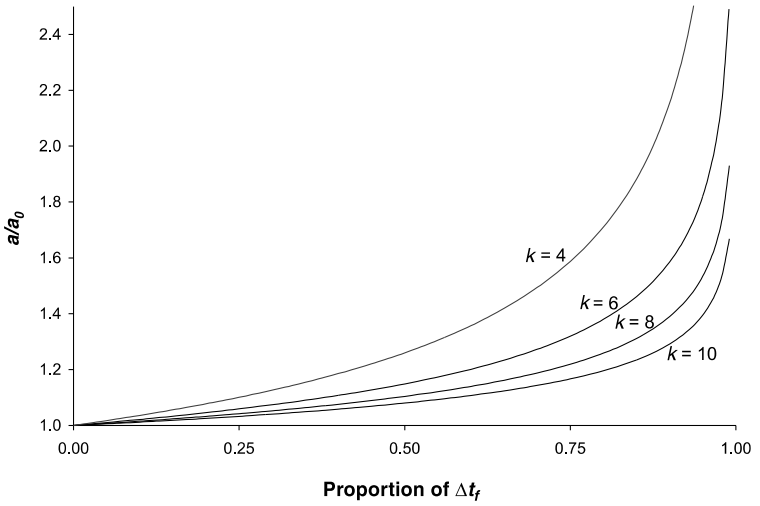

Fig. 27. Time-dependent crack growth at constant stress during period of instability.

$$\frac{a}{a_0} = \left[1 - \left(\frac{\Delta t}{\Delta t_f}\right)\right]^{\frac{-1}{k-1}}, \tag{12}$$

where a_0 and a are the initial and current (at time Δt) crack semi-lengths and Δt_f is a constant with units of time (see Ref. [13] for details). This relationship is plotted in Fig. 27 for various k; it can be seen that the crack instability is well captured. Further work is required to determine the various constants for ice.

5.1. Spalls and other splitting events

The spalls that occur near a high-pressure zone and run to a free surface were first considered by Croasdale [26] and Croasdale et al. [27] together with associated variations in load. There are a great variety of spall fractures; bigger ones, smaller ones, all with their effect on the applied load. It seems important to investigate the most important flaws in the material, and their likely influence in terms of spall and fracture initiation. It is certain that probabilistic aspects need consideration in order to account for the immense variation in observed loads and pressures. It seems natural that a high-pressure zone is likely to be associated with localized spalls; larger splits might be the result of the combined action of several high-pressure zones. Before carrying out the probabilistic analysis, a deterministic analysis of the most likely scenarios is appropriate. Zou et al. [76] considered the likely position of critical flaws in a beam-like structure. Likely candidates were grain boundaries under shear near the edges of a high-pressure zones. Recently Xiao [66] and Dempsey et al. [77] also considered this issue. It is observed that high-pressure zones move about continually; big spalls and splits take place from time to time. These occurrences emphasize the importance of treating the randomness with probabilistic methods.

Some researchers suggest that the macrocracks propagate from microcracks in the crushed and damaged layer. If one considers a single high-pressure zone, the central part is not distinguished by many cracks in the layer because of the high pressure. The outer edges contain microcracks but these are in the highly softened part of the layer that slips past the "undamaged" ice along the pulverization front. A crack passing through does not seem likely. At the same time, the shear that results from the mismatch in viscous properties needs to be considered, and has indeed been in our finite element simulations. Most likely sources remain the flaws and grain boundaries outside the layer.

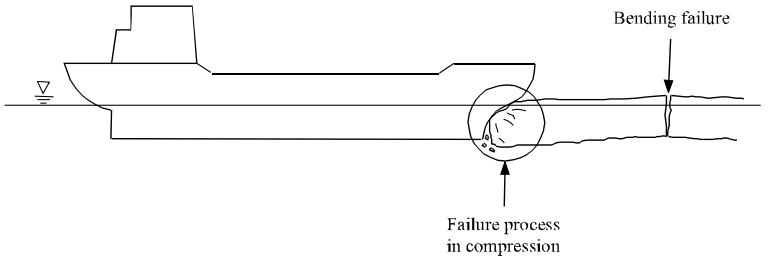

Fig. 28. Ship ramming an ice floe.

5.2. Fractures induced by geometry

In this section two examples of practical issues are introduced. The first concerns a ship inducing flexural failure (Fig. 28). The formula generally used in the case of ships for the force F at which flexural failure occurs is as follows:

$$F = c_f \sigma_f h^2, \tag{13}$$

where $c_f =$ parameter that accounts for the time-dependent flexural failure of ice, $\sigma_f =$ flexural strength (MPa), and $h =$ ice thickness. The equation would be appropriate for large plates, as dimensions other than thickness are not taken into account. We do note that the failure load corresponding to radial cracking including the effects of closure [78] varies as $h^{3/2}$; but it is noted that radial cracking is supposed to precede failure of the ''wedges'' so created, as proposed by Nevel [79]. The approach is summarized by Michel [80]; see also Ref. [71]. It is worth noting that one set of model tests suggests that the maximum load in tests using an inclined plane corresponds to radial cracking [81]. Hydrodynamic effects are also very important, but will not be considered further here. The question of the power to which h should be raised will be discussed again at the end of the present section.

The formula (13) has a considerable history of use in ice engineering [9]; at the same time, calibration of the values of c_f and σ_f presents real difficulties because of lack of full scale verification. An interesting result was obtained when simulating the loads in the Oden North Pole voyage. At first, the loads obtained using an ice crushing model did not show good agreement with the data since the ice was thin enough to permit flexural failure; this was shown in Fig. 4 (lower right). Inclusion of a failure model based on Eq. (13) with random flexural strength did indeed improve considerably the agreement, as shown in Fig. 29.

For the Confederation Bridge, a detailed method of analysis was used [21,82]. This included models for flexural failure of the ridge cores with associated ride up and clearing, together with failure of the ridge keels. There were inevitably some approximations, and a comparison was made with results of detailed measurements on the Kemi lighthouse in Finland [83]; see Fig. 30. There had been several years of detailed measurement. The analysis was in this case made for three ice thicknesses: thin ice (0.4–0.5 m), late winter ice (0.7–0.8 m) and rafted ice (1.1–1.3 m). The model developed for the Confederation Bridge was adjusted to match the details of the Kemi structure and the local environment.

Fig. 31 [82] shows a comparison of peak loads; the simulation method developed for the Confederation Bridge was used with best estimates for the parameters such as ice thickness, including variability. It should be emphasized that the Kemi experiment was closely monitored with detailed measurements of key parameters. The results in Fig. 30 show that the simulation method agrees well, but tends to overestimate in the extreme loads. This suggests a strong need for better and more realistic ice strength models (further details are given in Ref. [21]).

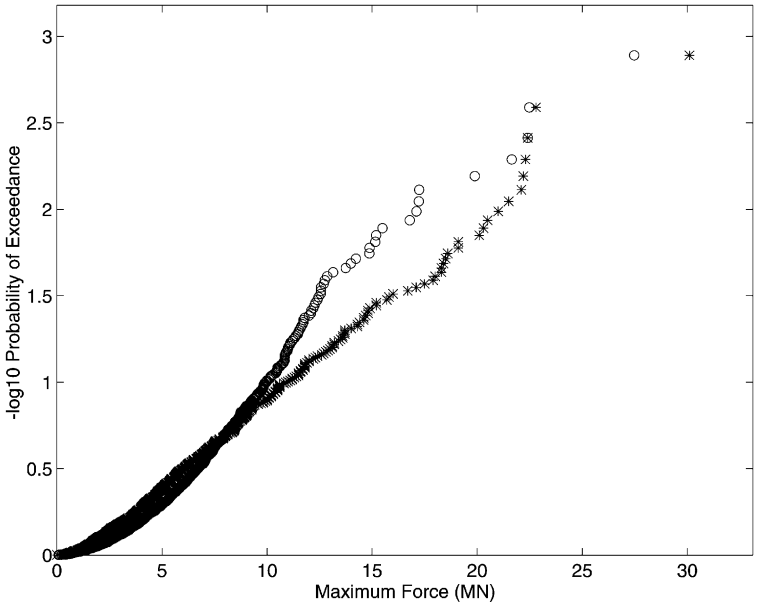

Fig. 29. Measured ship loads compared to simulation with inclusion of flexural failure: Oden North Pole voyage. Circles represent observations, crosses the simulation. See also Fig. 4, in which flexural failure was not considered.

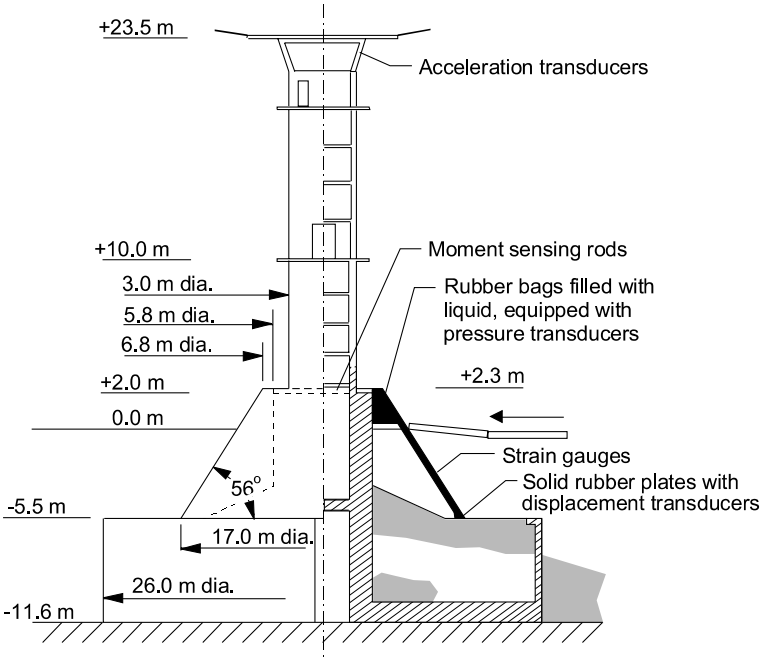

Fig. 30. Kemi-1 lighthouse [83].

A further point should be made. Määttänen et al. [84] discuss the relationship between maximum level ice force and thickness h, based on his experiments. They conclude that the dependence of ice force on h is

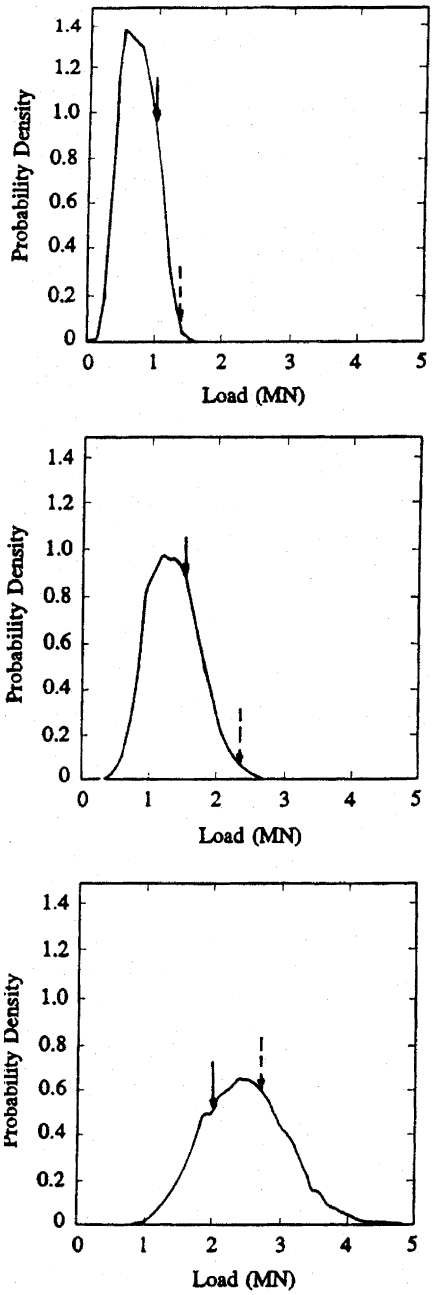

Fig. 31. Comparison of simulation (plotted as a density) with Kemi lighthouse measurements for three ice thicknesses. Solid and dashed arrows indicate mean and maximum peak loads respectively.

closer to a power of one than two. This conclusion was made notwithstanding the fact that it would be expected that rafted ice might have a lower failure strength than ice made of a single frozen layer; this fact was taken into account by the authors.

6. Discussion and concluding remarks

No analysis can match reality in all its complexity. From the standpoint of the designer of ice interactions with offshore structures, it is important to keep one's eye on the "real" situations. Strain rates can be very high, with values reaching many units per second in faster interactions, for example in ship-ice impacts. Although the average compressive stress may be quite low, of the order of 1 MPa or less, stresses in localized regions can be as high as 70 MPa. The ice would be highly confined, with hydrostatic pressures of this order. The medium scale tests provided invaluable information on the failure processes in compression. Yet we know that the ice, being some distance from the boundary of the sheet, was less prone to spall failures than other locations near the edges. Further, the interaction velocity was rather slow compared to some situations of interest, such as ship rams. It is necessary to consider how things might change with higher velocities. One might expect that the damaged zone would be more developed in the case, with the higher power input into the ice. With regard to the full scale, a good example of the insights that can be achieved is given by Brown et al. [85] and Morsy and Brown [86]. They performed interesting analyses of the Molikpaq interaction events, with models that take into account viscous effects and extrusion in the ice. The effect of structural compliance was dealt with, and the conclusions are of great importance to those studying the problem of ice–structure dynamics. Their results indicated that it is preferable to include terms for the viscous extrusion of the ice on the upswing in load; in the medium scale and in laboratory tests, the movement is often small (and even difficult to measure in laboratory tests). When crushed ice is being extruded from a 7 m thick ice floe, one would expect continuous extrusion; as discussed in the present paper, the structural movements are likely to be a smaller proportion of the relative interaction distance per cycle than in the laboratory (particularly with flexible indentors). Morsy and Brown [86] showed the importance of the structural deformation in the cyclic loading process (phase-lock); see also the analysis in Ref. [44].

The consideration of fracture mechanics is an essential aspect in the scale effect. We have attempted in the paper to show that the pressure–area relationship, and the randomness of full scale results, result from fracture processes. Probabilistic failure theories need to be developed and applied, based on deterministic analyses of the fracture process. The size and spatial density of flaws are the random quantities of interest. The work of Maes [87] is important in this regard, and needs to be taken further. Ice sheets of one or two metres thickness often split through the centre with a planar crack parallel to the surfaces of the plate, causing a cleavage fracture. (This is an occurrence well known to engineers detailing reinforcement for a prestressed plate.) The cracks generally will soon run to a free surface, but the contact area and position of the high-pressure zones are affected.

An individual high-pressure zone will fail at a distinct load. This load corresponds to failure of the layer of material at the boundary of the high-pressure zone, accompanied by ejection of crushed ice. The failure load is also random, depending on size; the failure process may be interrupted by fracture events. One can speculate on the effect of the interaction rate on the nature of high-pressure zones. As previously noted, faster rates lead to greater stress concentrations and consequently more spalls. These have a higher random component, and would tend to change position frequently. Possibly the "blue zones" would be less in evidence (or of shorter duration) than at lower rates, since more energy is being transferred into the ice (compare, for example the dropped ball tests). Certainly there is evidence of "continuous crushing" at high rates rather than the oscillation in load found at intermediate rates [29,88].

Apart from issues related to design, based on full scale experience as just outlined, it is important to continue fundamental studies of ice behaviour. Under high states of stress, ice shows a strong tendency to alter its microstructure. These changes result in changes of orders of magnitude in the compliance. The considerable softening that results has an analogy in geophysics in mylonite formation near fault zones. Thermal calculations and analysis need to be extended. Some ideas along these lines were presented in Ref. [47]. The work of Gagnon and Sinha Ref. [89] had shown that the temperature at the interface between the

ice and an indentor in medium scale testing decreases on the upswing in load. This we interpreted [52] as a "borrowing" of heat by the ice in order to melt under pressure. We calculate the melted volume as about 0.5% of the total volume involved in the melting process, based on the temperature change; the melted ice would in this interpretation be interspersed and concentrated at the grain boundaries [52]. In the medium scale tests about 7.5 kJ is consumed per load cycle. This would be consumed by viscous processes, and frictional effects. A rough calculation, on the assumption that the viscous layer is 0.02 m^3 in volume (0.2 $m^2 \times 0.1$ m thick) then this energy would result in a warming of the ice of about 0.2°, roughly in accordance with the measurements presented in Ref. [89]. Process zones in fracture need to be investigated, in terms of microstructural changes and consequent behaviour.

Gagnon and Sinha [89] and Gagnon [90] performed interesting experiments associated with the medium scale tests. These provided valuable information on the temperature variation during the indentation, melting under pressure, and on the examination of the visual information obtained by photography through a Lexan window. The role of the thinner areas of damaged ice in the extrusion process is emphasized. The results are consistent with the present analysis; the "cracks" and "spalls" in Refs. [89,90] are termed here the "pulverization front". Yet some of the statements made, particularly in Ref. [90], need to be qualified to put them in the context of the present paper. It is stated in Ref. [90] that "all damage to the ice, and actual movement of the indentor into the ice, occurred during the sharp drops in the sawtooth load data". With regard to the first of these (the movement of the indentor), a detailed analysis of the data shows that the actual deformation rate on the upswing is about half the programmed rate, because the servo-control device cannot follow exactly the programmed rate because of the surge following sudden drops in load (as already discussed – see Fig. 13). Indeed, Meaney et al. [36] show that a highly softened layer is needed to explain even this reduced rate. That damage occurs on the upswing in load is shown conclusively in the slower tests of the 1989 Hobson's choice series. The appearance of "regions of crushed ice" which "quickly grew in size" was actually noted in the paper [90]; these appeared early in the test. They would, in the context of the present paper, be considered as damage, so that damage was indeed observed on the upswing in load. Further, recrystallization under high confining pressure could occur as part of a "blue zone", not detectable by visual observation. Tests by Meglis et al. [49] show that under high confining pressures, this damaged ice is quite transparent. This kind of damage could quite easily (and has been observed to) occur on the upswing in load. At the same time, it would tend to occur at the highest pressures at the centre of extrusion, possibly just after the failure of the edges (Fig. 17).

Acknowledgements

The author acknowledges the helpful discussions with Ken Croasdale, John Dempsey, Bob Frederking and Max Coon, who suggested the use of phase-plane diagrams to illustrate the extreme regularity of the medium scale test results. John Pond and Paul Stuckey assisted immensely in the preparation of the paper. Financial support for the research from the Natural Sciences and Engineering Research Council of Canada, from the Government of Canada through the Program on Energy Research and Development, and from the Canada-Newfoundland Offshore Development Fund, is gratefully acknowledged.

References

[1] Jordaan IJ, McKenna RF, Duthinh D, Fuglem MK, Kennedy KP, Maes MA, Marshall A. Development of new ice load models. Report for Canada Oil and Gas Lands Administration (COGLA) by C-CORE, Memorial University, St. John's, NF, 1990, p. 206.
[2] Jefferies MG, Wright WH. Dynamic response of "Molikpaq" to ice–structure interaction. Proc 7th Int Conf Offshore Mech Arctic Engng 1988;IV:201–20.

[3] Frederking RMW, Jordaan IJ, McCallum JS. Field tests of ice indentation at medium scale: Hobson's choice ice island, 1989. Proceedings, 10th International Symposium on Ice 2, IAHR, Espoo, Finland, 1990. p. 931–44.
[4] Jordaan IJ, Xiao J. Compressive ice failure. In: Shen HT, editor. Ice in surface waters, Proceedings, IAHR Symposium on Ice, 1998. Potsdam, New York, 1999. p. 1025–31.
[5] Fuglem M, Muggeridge K, Jordaan IJ. Design load calculations for iceberg impacts. International Offshore and Polar Engineering Conference, vol. 2. Montreal, Canada, 1998. p. 460–67; Int J Offshore Polar Engng 1999;9(4):298–306.
[6] Jordaan IJ. Experience using probabilistic methods in problems of the Canadian frontier. In: Melchers RE, Stewart MG, editors. Applications of statistics and probability, Proceedings of the ICASP 8 Conference, Sydney, Australia, 1999. Balkema, 2000. p. 1219–26.
[7] Carter JE, Daley C, Fuglem M, Jordaan IJ, Keinonen A, Revill C, Butler T, Muggeridge K, Zou B. Maximum bow force for arctic shipping pollution prevention regulations – phase II. Ocean Engineering Research Centre, Memorial University of Newfoundland, submitted to Canadian Coast Guard, Arctic Ship Safety, 1995. p. 247.
[8] Canadian Standards Association, 1992. General requirements, design criteria, the environment, and loads. Standard CAN/CSA-S471-92.
[9] Fuglem M, Jordaan IJ. Estimation of maximum bow force for arctic vessels. In: Shen HT, editor. Proceedings, IAHR Symposium on Ice, 1998. Potsdam, New York, 1999. p. 947–55.
[10] Cowper B, Edgecombe M. The 1985 global ice impact tests on the USCG Polar sea. Transport Canada Development Centre, 1987, TP8496E.
[11] Edgecombe M, St John JW, Liljestrom G, Ritch A. Full scale measurement of hull-ice impact loads and propulsion machinery response onboard I/B Oden during the 1991 international arctic ocean expedition. Canadian Coast Guard Northern, 1992, TP11252E.
[12] Masterson DM, Spencer PA, Nevel DE, Nordgren RP. Velocity effects from multiyear ice tests. Proceedings, 18th International Conference on Offshore Mechanics and Arctic Engineering (OMAE99). St. John's, Canada, 1999.
[13] Jordaan IJ, Xiao J. Interplay between damage and fracture in ice–structure interaction. Proceedings of the 11th International Symposium on Ice, vol. 3. Alberta, Canada, 1992. p. 1448–67.
[14] Jordaan IJ. Probabilistic analysis of environmental data for design of fixed and mobile arctic offshore structures. Reliability and risk analysis in civil engineering. Proceedings of ICASP5, the Fifth International Conference on Applications of Statistics and Probability in Soil and Structural Engineering, vol. 2. Vancouver, BC, 1987. p. 1130–37.
[15] Jordaan IJ, Maes MA, Brown PW, Hermans IP. Probabilistic analysis of local ice pressures. J Offshore Mech Arctic Engng 1993;115:83–9.
[16] Brown PW, Jordaan IJ, Nessim MA, Haddara MMR. Optimisation of bow plating for icebreakers. J Ship Res Soc Naval Architects Marine Engrs 1996;40(1):70–8.
[17] Sanderson TJO. Ice mechanics: risks to offshore structures. Graham and Trotman: 1988.
[18] Jordaan IJ, Fuglem M, Matskevitch DG. Pressure–area relationships and the calculation of global ice forces. Proceedings, IAHR Symposium on Ice. vol. 1. Beijing, China, 1996. p. 166–75.
[19] Fuglem M, Jordaan IJ, Crocker G. Iceberg-structure interaction probabilities for design. Can J Civil Engng 1996;23(1):231–41.
[20] Carter JE, Frederking RMW, Jordaan IJ, Milne WJ, Nessim MA, Brown PW. Review and verification of proposals for the arctic shipping pollution prevention regulations. Ocean Engineering Research Centre, Memorial University of Newfoundland, submitted to Canadian Coast Guard, Arctic Ship Safety, 1992.
[21] Brown TG, Jordaan IJ, Croasdale KR. Probabilistic analysis of ice loads for the Confederation Bridge. Can J Civil Engng (in press).
[22] Kry PR. A statistical prediction of effective ice crushing stresses on wide structures. Proceedings of the 5th International IAHR Conference, Part 1. Lulea, Sweden, 1978. p. 33–47.
[23] Ashby MF, Palmer AC, Thouless M, Goodman DJ, Howard M, Hallam SD, Murrell SAF, Jones N, Sanderson TJO, Ponter ARS. Nonsimultaneous failure and ice loads on arctic structures. Offshore Technology Conference, 1986. p. 399–404.
[24] Blanchet D, DeFranco SJ. Global first-year ice loads: scale effect and non-simultaneous failure. Proceedings of the 14th International Symposium on Ice. Beijing, China, 1996. p. 203–13.
[25] Glen IF, Blount H. Measurements of ice impact pressures and loads onboard CCGS Louis S. St. Laurent. In Proceedings, 3rd Offshore Mechanics and Arctic Engineering Symposium, vol. III . ASME, New Orleans, LA, 1984. p. 246–52.
[26] Croasdale KR. Ice forces on marine structures. Proceedings, Third International Symposium on Ice Problems. IAHR, Hanover, NH, 1975. p. 315–37.
[27] Croasdale KR, Morgenstern NR, Nuttal JB. Indentation tests to investigate ice pressures on vertical piers. J Glaciology 1977;19(81):301–12.
[28] Riska K, Rantala H, Joensuu A. Full scale observations of ship–ice impact. Helsinki University of Technology, Report M-97, 1990.
[29] Singh SK, Jordaan IJ, Xiao J, Spencer PA. The flow properties of crushed ice. Trans ASME 1995;117:276–82.
[30] Jordaan IJ, Xiao J, Zou B. Fracture and damage of ice: towards practical implementation. Proceedings, 1st Joint Mechanics Meeting of ASME. ASCE, SES, Charlottesville Virginia 1993;AMD163 (Ice Mechanics):251–60.

[31] Johnston ME, Croasdale KR, Jordaan IJ. Localized pressures during ice–structure interaction: relevance to design criteria. Cold Regions Sci Technol 1998;27:105–17.
[32] Zou B. Ships in ice: the interaction process and principles of design. PhD Thesis, Memorial University of Newfoundland, 1996.
[33] Masterson DM, Nevel DE, Johnson RC, Kenny JJ, Spencer PA. The medium scale iceberg impact test program. Proceedings, IAHR Ice Symposium. Banff, Alberta, 1992.
[34] Masterson DM, Frederking RMW, Jordaan IJ, Spencer PA. Description of multi-year ice indentation tests at Hobson's Choice Ice Island – 1990, Proceedings, 12th International Conference on Offshore Mechanics and Arctic Engineering, vol. 4. Glasgow 1993. p.145–55.
[35] Jordaan IJ, Timco GW. The dynamics of the ice crushing process. J Glaciology 1988;34(118):318–26.
[36] Meaney R, Jordaan IJ, Xiao J. Analysis of medium scale ice-indentation tests. Cold Regions Sci Technol 1996;24:279–87.
[37] Kennedy KP, Jordaan IJ, Maes MA, Prodanovic A. Dynamic activity in medium-scale ice indentation tests. J Cold Regions Sci Technol 1994;22:253–67.
[38] Sinha NK, Cai B. Analysis of ice from medium-scale indentation tests. National Research Council of Canada, Institute for mechanical Engineering, Laboratory Memorandum 1992-2.
[39] Kenny S, Meaney R. Failure zone characterization: medium-scale field indentation program Hobson's choice ice island 1990. Memorial University of Newfoundland, 1991.
[40] Ochi MK. Applied probability and stochastic processes. Wiley; 1990.
[41] Spencer PA, Masterson DM, Lucas J, Jordaan IJ. The flow properties of crushed ice: experimental. Proceedings, IAHR Symposium on Ice, vol. 1. Banff, Alberta, 1992. p. 258–68.
[42] Schulson EM. An analysis of the brittle to ductile transition in polycrystalline ice under tension. Cold Regions Sci Technol 1979;1:87–91.
[43] Schulson EM. The brittle compressive fracture of ice. Acta Mettallurgica et Materiala 1990;38:1963–76.
[44] Jordaan IJ, Singh SK. Compressive ice failure: critical zones of high pressure. Proceedings 12th Int IAHR Ice Symp, vol. 1. Trondheim, Norway, 1994. p. 505–14.
[45] Barnes P, Tabor D, Walker JCF. The friction and creep of polycrystalline ice. Proc Roy Soc Lond A 1971;324:127–55.
[46] Kheisin DE, Cherepanov NW. Change of ice structure in the zone of impact of a solid body against the ice cover surface. Problems of the Arctic and Antarctic, 1970, Issues 33–35 (A.F. Treshnikov), Israel Program for Scientific Translations, 1973. p. 239–45.
[47] Xiao J, Jordaan IJ, Singh SK. Pressure melting and friction in ice–structure interaction. Proceedings, 11th IAHR International Ice Symposium, vol. 3. Banff, Alberta, 1992. p. 1255–68.
[48] Melanson P, Meglis I, Jordaan IJ, Stone BS. Microstructural change in ice: I. Constant deformation-rate tests under triaxial stress conditions. J Glaciology 1999;45(151):417–22 [colour plates 423–36].
[49] Meglis I, Melanson P, Jordaan IJ. Microstructural change in ice: II. Creep behavior under triaxial stress conditions. J Glaciology 1999;45(151):438–48 [colour plates 423–36].
[50] Muggeridge K, Jordaan IJ. Microstructural change in ice: III. Observations from an iceberg impact zone, J Glaciology 1999;45(151):449–55 [colour plates 423–36].
[51] Kurdyumov VA, Kheisin DE. Hydrodynamic model of the impact of a solid on ice. Prikladnaya Mekhanika 1976;12(10):103–9 [Transl.].
[52] Jordaan IJ, Matskevitch DM, Meglis I. Disintegration of ice under fast compressive loading. Proceedings of the Symposium on Inelasticity and Damage in Solids Subject to Microstructure Change, Memorial University of Newfoundland. 1997:211–31; Extended version, International Journal of Fracture 1999;97(1–4):279–300.
[53] Duthinh D. Pressure of crushed ice as Mohr–Coulomb material against flat, axisymmetric indentor. J Cold Regions Engng, ASCE 1992;6(4):139–51.
[54] Frederking RMW, Sayed M. Stress distribution as a reflection of failure processes during medium scale ice indentation. Proceedings, IAHR Symposium on Ice, vol. 3. Banff, Alberta, 1992. p. 1278–88.
[55] Stone BM, Jordaan IJ, Xiao J, Jones S. Experiments on the damage process in ice under compressive states of stress. J Glaciol 1997;43:11–25.
[56] Singh SK, Jordaan IJ. Constitutive behaviour of crushed ice. Proceedings of the Symposium on Inelasticity and Damage in Solids Subject to Microstructure Change, Memorial University of Newfoundland, 1997, p. 367–79; Extended version, International Journal of Fracture 1999;97(1–4):171–87.
[57] Jordaan IJ, Stone BM, McKenna RF, Fuglem MK. Effect of microcracking on the deformation of ice. Can Geotechnical J 1992;29:143–50.
[58] Sinha NK. Crack-enhanced creep in polycrystalline material: strain-rate sensitive strength and deformation of ice. J Mater Sci 1988;23:4415–28.
[59] Kachanov M. Proper parameters of defect density for solids with cracks and cavities. Proceedings of the Symposium on Inelasticity and Damage in Solids Subject to Microstructure Change, Memorial University of Newfoundland, 1997, p. 47–72. Extended version Solids with cracks and non-spherical pores: proper parameters of defect density and effective elastic properties in the Int J Fract 1999;97(1–4):1–32.

[60] Melanson PM, Jordaan IJ, Meglis IL. Modelling of damage in ice, In: Shen HT, editor. Proceedings, IAHR Symposium on Ice, 1998. Potsdam, New York, 1999, p. 979–88.
[61] Cole DM. A model for the anelastic straining of saline ice subjected to cyclic loading. Philos Mag A 1975;72(1):231–48.
[62] Schapery RA. On viscoelastic deformation and failure behaviour of composite materials with distributed flaws. Adv Aerospace Struct Mater ASME 1981;AD-01:5–20.
[63] Budiansky B, Hutchinson JW, Slutsky S. Void growth and collapse in viscous solids. In: Hopkins HG, Sewell MJ, editors. Mechanics of Solids, The Rodney Hill 60th Anniversary Volume. Oxford: Pergamon Press; 1982. p. 13.
[64] Jordaan IJ, McKenna RF. Processes of deformation and fracture of ice in compression. Proceedings IUTAM-IAHR Symposium on Ice–Structure Interaction, St. John's, Newfoundland, Canada, August 1989, Springer, 1991. p. 283–309.
[65] McKenna RF, Jordaan IJ, Xiao J. Damage and energy flow in the crushed layer during rapid ice loading. IAHR Symposium on Ice, vol. 3. Espoo, Finland, 1990. p. 231–45.
[66] Xiao J. Damage and fracture of brittle viscoelastic solids with application to ice load models. PhD Thesis. Memorial University of Newfoundland, 1997. p. 187.
[67] Sammonds PR, Rist MA. Sea ice fracture and friction. IUTAM Symposium on Scaling Laws in Ice Mechanics and Ice Dynamics. 2000.
[68] Gold LW. Crack formation in ice plates by thermal shock. Can J Phys 1963;41:1712–28.
[69] Palmer AC, Goodman DJ, Ashby MF, Evans AG, Hutchinson JW, Ponter ARS. Fracture and its role in determining ice forces on offshore structures. Ann Glaciol 1983;4:216–21.
[70] Timco GW, Frederking RMW. The effects of anisotropy and microcracks on the fracture toughness of freshwater ice. Proceedings OMAE, Tokyo, 1986.
[71] Dempsey JP. Research trends in ice mechanics. Research Trends in Solid Mechanics. USNC/TAM Committee, 1999.
[72] Dempsey JP, DeFranco SJ, Adamson RM, Mulmule SV. Scale effects on the in-situ tensile strength and fracture of ice. I: Large-grained freshwater ice at spray lakes reservoir, Alberta. II: First-year sea ice at resolute, NWT. Int J Fract, I, vol. 95, 1999, pp. 325–45;II pp. 347–66.
[73] Mulmule SV, Dempsey JP. A viscoelastic fictitious crack model for the fracture of sea ice. Mech Time-dependent Mater 1998;1:331–56.
[74] Dempsey JP. Scale effects on the fracture of ice. The Johannes Weertman Symposium. The Minerals, Metals and Materials Society, 1996. p. 351–61.
[75] Schapery RA. Simplifications in the behaviour of viscoelastic composites with growing damage. Proceedings of the IUTAM Symposium on Inelastic Deformation in Composite Materials. Troy (New York): Springer; 1991.
[76] Zou B, Xiao J, Jordaan IJ. Ice fracture and spalling in ice–structure interaction. Cold Regions Sci Technol 1996;24:213–20.
[77] Dempsey JP, Palmer AC, Sodhi DS. High pressure zone formation during compressive ice failure. Proceedings of the OMAE Conference, 1999.
[78] Dempsey JP, Slepyan LI, Shektman II. Radial cracking with closure. Int J Fract 1995;73:233–61.
[79] Nevel DE. The narrow infinite wedge on an elastic foundation. Cold Regions Research and Engineering Laboratory, Research Report 79, 1961.
[80] Michel B. Ice Mechanics, Laval, 1978.
[81] Frederking RMW, Timco GW. Quantitative analysis of ice sheet failure against an inclined plane. Proc 4th OMAE 1985;II:160–9.
[82] Cammaert AB, Jordaan IJ, Bruneau SE, Crocker GB, McKenna RF, Williams SA. Analysis of ice loads on main span piers for the Northumberland Strait crossing, contract report, J. Muller International–Stanley Joint Venture Inc., CODA contract number 5022.01, 1993.
[83] Määttänen M, Hoikkanen J. The effect of ice pile-up on the ice force of a conical structure. Proceedings, IAHR 10th International Symposium on Ice, vol. 2. Espoo, Finland, 1990. p. 1010–21.
[84] Määttänen M, Hoikkanen AN, Avis J. Ice failure and ice loads on a conical structure – Kemi-I cone full scale ice force measurement data analysis. Proceedings, 13th International IAHR Symposium on Ice, vol. 1. Beijing, China, 1996. p. 8–16.
[85] Brown TG, Wright BD, Rogers B, Jefferies M, Bruce JR. A model for dynamic interactions with Molikpaq. Proceedings of IAHR Ice Symposium, vol. 3. Banff, Alberta, June 1992. p. 1289–303.
[86] Morsy UA, Brown TG. Three-dimensional non-linear finite element model for the Molikpaq, Gulf's mobile arctic caisson. Comput Struct 1996;60(4):541–60.
[87] Maes M. Probabilistic behaviour of a Poisson field of flaws in ice subjected to indentation. Proceedings, 11th International IAHR Symposium on Ice, vol. 2. Banff, Canada, 1992. p. 871–82.
[88] Singh SK, Timco GW, Frederking RMW, Jordaan IJ. Tests of ice crushing on a flexible structure. Proceedings, International Conference on Offshore Mechanics and Arctic Engineering, vol. IV. Houston, TX, 1990. p. 89–94.
[89] Gagnon RE, Sinha NK. Energy dissipation through melting in large scale indentation experiments on multiyear sea ice. Proceedings, 10th International Conference on Offshore Mechanics and Arctic Engineering, vol. 4. Stavanger, 1991. p. 157–61.
[90] Gagnon RE. Analysis of visual data from medium scale indentation experiments at Hobson's Choice Ice Island. Cold Regions Sci Technol 1998;28:45–58.